



Novel Shade Dispersion Techniques for Reconfiguration of Partially Shaded Photovoltaic Arrays

Rayappa David Amar Raj^{1,2} · Kanasottu Anil Naik¹

Received: 12 April 2022 / Accepted: 25 January 2023 / Published online: 10 March 2023
© The Author(s), under exclusive licence to Springer Nature Singapore Pte Ltd. 2023

Abstract

The photovoltaic (PV) arrays are inevitably subjected to partial shading (PS) conditions that highly limit the output. To mitigate these effects, various reconfiguration procedures have been executed by the researchers. However, many of these procedures fail to disperse the shade effectively over the entire array and hence there is a dire need for such an efficient reconfiguration technique. This paper explores Knight's Tour Magic square (KTM) and Doubly Even-order Magic square (DEM) techniques which effectively disperse the shadow by reconfiguring the array without altering the electrical connections. To examine the superiority of the proposed techniques, their performance has been compared with conventional total-cross-tied, existing odd-even and odd-even-prime configurations of a symmetric 8×8 and asymmetric 4×3 PV arrays. Further, the applicability of the proposed techniques is proved by analysing the system with eight performance parameters such as global maximum power, power mismatch, percentage losses, efficiency, fill factor, capacity factor, array yield, and performance ratio under 20 distinct PS patterns. The power enhancement in GMP using the KTM and DEM approaches are nearly 42.67%, 17.87%, 16.24%, 8.04% for asymmetric arrays, and 26.43%, 25.38%, 25.09%, 15.61%, 10.63%, for the symmetric arrays. Finally, a comprehensive economic analysis is also performed, and it is observed that there is a significant augmentation in the number of units and the revenue generated by employing the proposed techniques.

Keywords PV array · Partial shading · Reconfiguration · Shade dispersion · Mismatch

Abbreviations

BL	Bridge-linked	M	Magic constant
CF	Capacity factor	N	Magic square order
IV	Current voltage	MPPT	Maximum power point tracking
DEM	Doubly even-order magic square	P	Parallel
FF	Fill factor	PR	Partial shading
GA	Genetic algorithm	PS	Performance ratio
GMP	Global maximum power	PV	Photovoltaic
HC	Honeycomb	PV	Power voltage
IE	Irradiance equalization	S	Series
KTM	Knights tour magic square	SB	Series parallel
LB	Long broad	SN	Short broad
LN	Long narrow	SP	Short narrow
		STC	Standard test conditions
		OE	Odd even
		OEP	Odd even prime

✉ Rayappa David Amar Raj
dctdavid2k15@gmail.com

Kanasottu Anil Naik
anilnaik205@nitw.ac.in

¹ Department of Electrical Engineering, National Institute of Technology, Warangal, Telangana, India

² Department of Electrical Engineering, National Institute of Technology Warangal, Warangal, India

Parameters

TCT	Total-cross-tied
Y_{array}	Array Yield
V_{pv}	Cell voltage
$E_{dc, array}$	DC energy of array
I_D	Diode current
α	Diode ideality factor

η	Efficiency
E_{actual}	Energy generated
GMP_{shaded}	GMP under shaded conditions
GMP_{unshaded}	GMP under unshaded
MMP	Mismatch Power
I_o	Reverse saturation current
P_L	Percentage power loss
I_{ph}	Photon-current generated
$P_{\text{pv,rated}}$	Power output (rated)
I	PVcell output current
A	PV panel area
R_s	Series resistance
R_{sh}	Shunt resistance
G	Solar irradiation
V_T	Thermal voltage

Introduction

Partial shading greatly limits the PV array output and will in turn leads to the development of hotspots in the PV array which further directs to dangerous fire hazards and ultimately destroys the module [1]. To safeguard the module, a bypass diode should be installed across it and these diodes bypass the current during low irradiations [2]. Nonetheless, the installation of these diodes instigates various peaks in an array characteristics. Another popular technique to reduce the impacts of PS is by installing maximum power point tracking (MPPT) controllers in the array [3]. However, these controllers necessitate complicated power converters and various control algorithms for operation. Despite its effectiveness in tracking the maximum power during PS, using these controllers increases the complexity, overall system cost. Due to the limitations of MPPT controllers, the reconfiguration methods are regarded as the best alternative to overcome the above-said limitations [4].

The reconfiguration methods are categorized as static and dynamic reconfiguration methods. Some of the notable dynamic reconfiguration techniques in the literature are presented as follows: The authors in [5] validated a completely dynamic PV array reconfiguration scheme that employs a neuro-fuzzy methodology and a switch matrix to regulate the configuration of the electrical array. The PV array reconfiguration strategy that depends on the short-circuit current evaluated by a convolutional neural network (CNN) under PS Conditions is proposed in [6]. An Irradiance Equalization (IE) concept-based reconfiguration procedure is proposed in [7] by reconfiguring the array in such a way that the summation of irradiation received by the modules in all the rows of an array must be made equal. In contrast to the principle of IE where the array output is enhanced solely by increasing the row current without regarding the array voltage, the authors in [8] proposed a 0/1 Multi knapsack problem based optimized

dynamic reconfiguration approach by directly estimating the global maximum power (GMP) of the array. In [9], the authors experimentally verified an intelligent reconfiguration scheme based on the Fuzzy logic system. The optimized configuration is calculated by fuzzy system and the result is later implemented to reconfigure the modules by using a switching matrix. Nevertheless, this approach demands numerous steps and complex circuitry.

Enhancing the solar PV power generation with the metaheuristic-based grey wolf optimizer for array reconfiguration under various scenarios has been invested in [10]. The authors in [11], developed an enhanced immune genetic algorithm to reconfigure the thermoelectric power generation system under nonuniform temperature distribution conditions in order to optimize power output. By developing a modified form for the simple hunger games-search optimizer, the authors in [12] proposed a novel hunger games search optimization approach-based array reconfiguration to reach optimal diversity and robust utilization of the best solutions. These dynamic reconfiguration approaches enhance the output during PS; however, they require many complicated switches and algorithms to administer these switches, complex controlling units, efficient driver circuits and sensors, systematic monitoring units which makes the system entirely intricate and also uneconomical. For an instance, it is reported in [13] that the number of switches obliged to dynamically reconfigure a simple 9×9 PV array is 1384. To evade the above complexities of dynamic approaches, static reconfiguration techniques are preferred.

A static reconfiguration method based on Sudoku-puzzle is proposed in [14] to distribute the shadow in the array to lessen the shading losses. The above sudoku-puzzle is further developed by the authors in [15] and obtained an optimal-sudoku approach to alleviate the mismatch. Despite its effectiveness, the Sudoku-puzzle is implemented for only 9×9 PV arrays. Moreover, the Sudoku-puzzle contains numerous sets of solutions, and obtaining the optimal reconfigured pattern is a great challenge. Furthermore, in some instances, effective shade dispersal is also not assured. A Ken-Ken-square puzzle-based configuration is proposed in [16] for 6×6 array to yield more power and reduce wiring losses compared to Sudoku technique. To minimize the power losses caused due to PS, the authors in [17] proposed an Odd-even (OE) pattern-based reconfiguration strategy for a simple 6×4 PV array. An enhanced version of the OE-based reconfiguration strategy named odd-even-prime (OEP) strategy has been proposed in [18] to be employable for both symmetric and asymmetric sizing of PV arrays. In contrast to the numerous existing strategies, the OEP strategy mitigates the row current mismatch of the asymmetric PV arrays as well. An innovative Zigzag strategy-based reconfiguration has been executed on a 4×3 PV array to replace the modules for increased shade dispersal [19]. However, first column in an array remains unchanged.

Most of the recommended reconfiguration strategies are not implementable for both symmetrical and non-symmetrical PV arrays. To redress this, a novel reconfiguration procedure based on Skyscraper-puzzle has been executed in [20] to augment the GMP and to lessen the line losses. A Polycube puzzle-based Dancing-Links algorithm is presented for solving a 6×6 Sudoku-puzzle [21]. To verify the practical viability of the proposed algorithm, a shifting cloud pattern regarding the direction and speed of wind with discrete instants has been analysed. The authors in [22] introduced a reconfiguration scheme based on a Magic-Square puzzle by using a genetic algorithm (GA) toolbox in MATLAB. A one-time reconfiguration approach based on Lo-Shu magic square is suggested in [23]. An Optimized fixed reconfiguration is exercised in [24] to alleviate the impacts of mutual shading independent of factors of shading such as sun's location, system's latitude, and the installation viewpoints of PV array.

To mitigate the row currents mismatch, the authors in [25] proposed an arrow-sudoku puzzle-based reconfiguration scheme for a 6×6 PV array. A tom-tom puzzle-based reconfiguration scheme is proposed for a small 5×5 PV to physically rearrange the panels for equalizing the irradiation levels of the rows in an array [26]. To examine the efficacy of Arrow-Sudoku and Tom-Tom puzzle-based schemes, they were tested under few growing dynamic PS patterns. The authors in [27] proposed an approximately balanced dispersal of shaded panels in distinct rows of a small 4×4 PV array by employing a diagonally-distributed-TCT reconfiguration scheme. A new column index strategy has been developed in [28] to determine the fixed configuration of the array by physically relocating the panels. Very recently, the authors in [29, 30] have employed two chaotic map-based techniques such as chaotic baker map and henon map for PV array reconfiguration to enhance the array characteristics and mitigate the multiple power peaks. However, both these approaches fail significantly under diagonal and column type shading conditions. Further, both these strategies are not scalable for asymmetric PV arrays.

It is deduced that static reconfiguration techniques are simple, cost-effective, reliable and competent. However, some of the above-mentioned reconfiguration techniques cannot rearrange the elements in first-column and hence fail to disperse the first-column shade and thus providing a sub-optimal solution under PS. Further, only a few of these techniques are compatible with the asymmetrical and large-rated arrays. As a result, the development of an optimal reconfiguration of large-rated arrays for effective shade dispersion remains as a major research gap. The primary challenges related to the present work are as follows:

- The methodologies employed in the dynamic reconfiguration procedures [5–13] are complicated and include weighted-sum methodology, early convergence issues,

difficult searching mechanisms, increased processing complexity, optimised weights determination, difficult parameter tuning, multiple stages to obtain solutions, etc.

- These dynamic strategies require a significant number of sensors and switches, complicated switching matrices, driver circuits, micro-controllers, etc. to implement, which raises substantial practical and financial concerns.
- Numerous static approaches [14–16, 19–29] now in use are inapplicable to asymmetric arrays and are primarily compatible with a small number of symmetrical PV array sizes. In reality, the majority of existing PV arrays are asymmetrical. Finding the best puzzle-based and logic-based strategy from the infinite solution sets is a very time-consuming process.
- The existing reconfiguration algorithms yield poor shade dispersion, which underperforms in some scenarios due to uneven shade dispersion, increased mismatch, unreliable performance, low power improvement, and inconsistent performance.
- Further, the existing techniques demonstrate several local power maxima in the array characteristics despite increasing GMP to some extent. Since the array's global maximum power needs to be tracked, this imposes a significant strain on the MPPT controllers and ends up making expensive, advanced MPPT controllers necessary.

To rectify the above setbacks, two novel reconfiguration techniques are proposed in this paper to disperse the shading effectively over the entire PV array under PS. The major contributions of this paper are as follows:

- In this paper, a Knight's Tour Magic square (KTM) and Doubly Even-order Magic square (DEM) approaches are proposed to effectively disperse the shade over the entire array thereby reducing the mismatch losses.
- To demonstrate the potency of the proposed techniques, their performance has been examined with the conventional total-cross-tied [2, 31], odd-even [17], odd-even-prime [18] configurations extensively analyzed under 20 distinct PS patterns.
- The performance of the considered strategies is investigated with five performance parameters such as global maximum power, power mismatch, percentage losses, efficiency, and performance ratio.
- A majority of the other contemporary strategies are compatible only for symmetrical array sizes and hence they are not validated/ tested for the unsymmetrical array sizes. However, the proposed strategies are scalable for both symmetrical and unsymmetrical arrays. The proposed KTM and DEM approaches are tested for a symmetric 8×8 and asymmetric 3×4 PV arrays.
- Additionally, a comparative economic analysis of the proposed KTM and DEM configurations with the con-

ventional TCT configuration has been performed to demonstrate the associated economic benefits. The electricity units generated, revenue yielded, and the payback obtained for the considered array configurations are assessed and investigated.

- The detailed comparative analysis of the proposed KTM and DEM approaches with the other recently reported state-of-art strategies has been performed in detail.

Modelling of Solar Cell

Several approaches for modeling a PV cell are published in the literature as follows: one-diode, two-diode, and three-diode models [32]. In this work, a one-diode equivalent circuit model is employed due to its simplicity as shown in Fig. 1.

By using KCL at the junction ‘N’, the PV cell output current (I) is obtained as follows,

$$I = I_{ph} - I_D - \frac{V_{PV} + IR_s}{R_{sh}} \quad [31] \tag{1}$$

$$\text{where } I_D = I_0 \times \left[\exp\left(\frac{V_D}{\alpha V_T}\right) - 1 \right] \tag{2}$$

Here, ‘ I_{ph} ’ is photon-current generated, ‘ I_D ’ is diode current, ‘ R_s ’ and ‘ R_{sh} ’ are series and shunt resistances, ‘ V_{pv} ’ is cell voltage and ‘ I ’ is cell current, ‘ I_0 ’ is module reverse saturation current, ‘ α ’ is diode ideality factor and ‘ V_T ’ is thermal voltage.

Conventional PV Array Configurations

Some of the notable conventional array configurations reported in the literature are Series (S), Parallel (P), Series-Parallel (SP), Honey-Comb (HC), Bridge-linked

(BL), and Total-Cross-Tied [33]. The TCT configuration shown in Fig. 2 is preferable over other configurations due to following reasons: increased GMP, enhanced array characteristics, better output and reduced mismatch losses during PS, extensive employment in practical applications, better reliability [33]. Despite its effectiveness over other configurations under PS, TCT configuration has major setback as it doesn’t disperse the shadow and curtails the output. Therefore, there is a desperate necessity for array reconfiguration for efficient shade dispersal during PS.

Proposed Methodologies

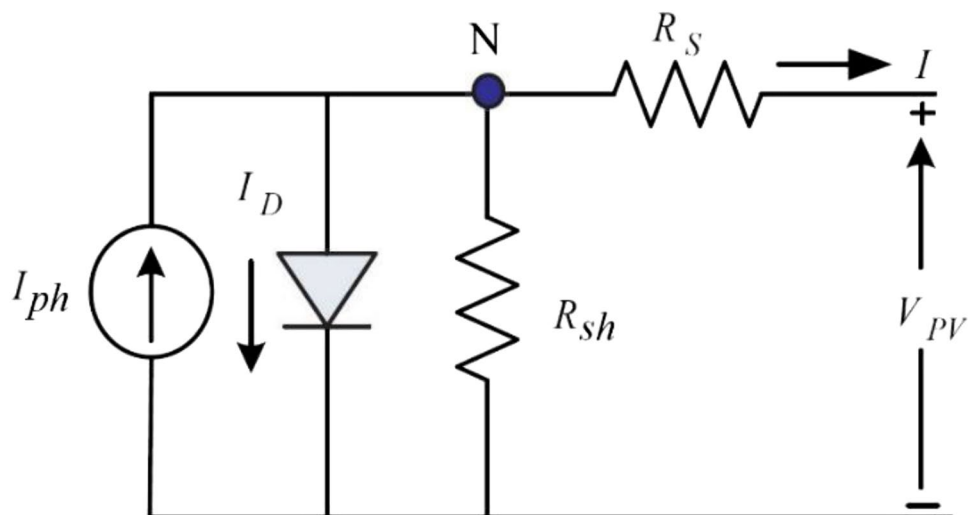
To attain effective shade dispersal through reconfiguration, the following techniques are employed:

Knight’s Tour Magic Square (KTM)

Knight’s Tour Magic square (KTM) is a semi-magic square proposed by Leonhard Euler in 1759. The reason why it is called a semi-magic square is: Firstly, all the numbers in each row and column add up to give 260. Secondly, all the numbers in each 4×4 sub-matrix add up to give 130 [34]. The chess knight is enabled to travel in L-direction on a chessboard whose squares are enumerated from 1 to 64 along the knight’s pathway, i.e., the first cell is designated as “1,” the following cell it visits is designated as “2,” and so forth as shown in Fig. 3(b). Here the pathway is termed as a tour if the knight moves about the chessboard in a general way (one vertical move and two horizontal moves or the other way round).

According to the knight’s tour problem, the knight is moved in such a way that it should visit all the cells in the chessboard only once. So, the main constraints of this

Fig. 1 Equivalent circuit of PV cell



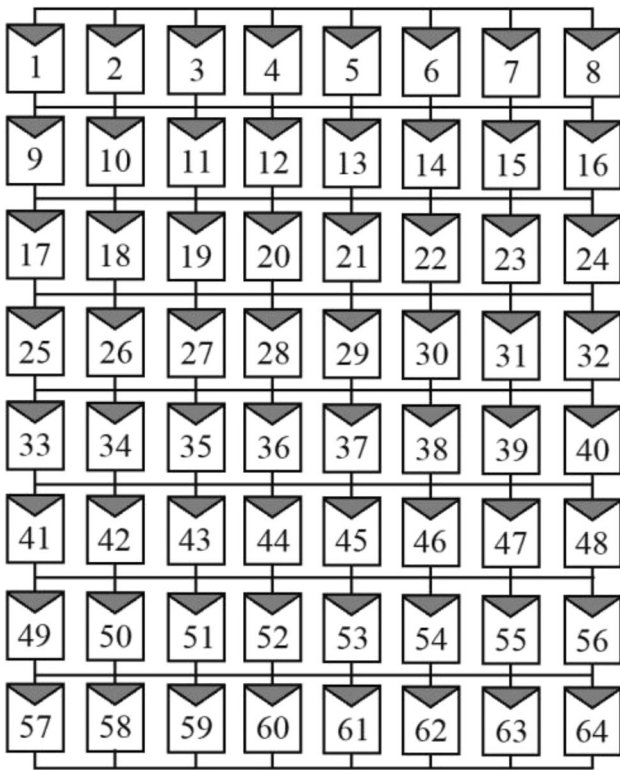


Fig. 2 TCT configurations of an 8×8 PV array

problem are: (a) each cell must be visited only once and (b) the knight should not overpass the board. These constraints can be solved by employing a recursive backtracking algorithm. It is executed to redirect the knight’s move when there doesn’t exist any further possible moves and also if not all the cells have been toured [35]. The chess knight follows closed tour and open tour approaches while moving. In closed tour approach, the knight returns to its original starting point after visiting each cell only once. However, in an open tour

approach which is employed in this work, the knight just visits all the cells but will not return to the starting point. An 8×8 matrix and its obtained Knight tour’s magic square matrix is shown in Figs. 3(a) and 3(b) respectively.

Doubly Even-Order Magic Square (DEM)

A magic square of order $N \times N$ contains the numbers numbered from 1 to N^2 are positioned in such a way that the sum of all the numbers in a row, in a column, and in the diagonal is the same. This constant numerical sum of all the numbers in a row or column or diagonal of the magic square is termed as a magic sum or magic constant [36]. For an 8×8 magic square, the magic constant is 260. Generally, the magic constant of any magic square can be determined by,

where M is magic constant, and N is order of the magic square. The magic squares are majorly classified on the basis of their order as follows: odd-order magic square with order $(2N + 1)$, then doubly even-order magic square with order $(4N)$, and finally singly-even magic square with order $(4N + 2)$, where $N = 1, 2, 3$ and so on [37]. In this paper, DEM approach is employed for reconfiguration. The obtained Doubly Even-order Magic square matrix is given in Fig. 4(b).


The step-by-step formulation of Doubly Even-order Magic square is as follows:

Step 1: Fill all the cells with numbers from 1 to N^2 (i.e. 1 to 64) sequentially in a row-wise manner.


Step 2: Draw two main diagonals of the square. Swap the blue-coloured diagonal numbers that are equally distant from the centre.

Step 3: Form a diamond-shaped 4×4 sub-square lines which pass through 16 red-coloured numbers as shown in Fig. 3(a).

Fig. 3 a An 8×8 matrix numbered from 1 to 64, b Obtained Knight tour’s magic square matrix

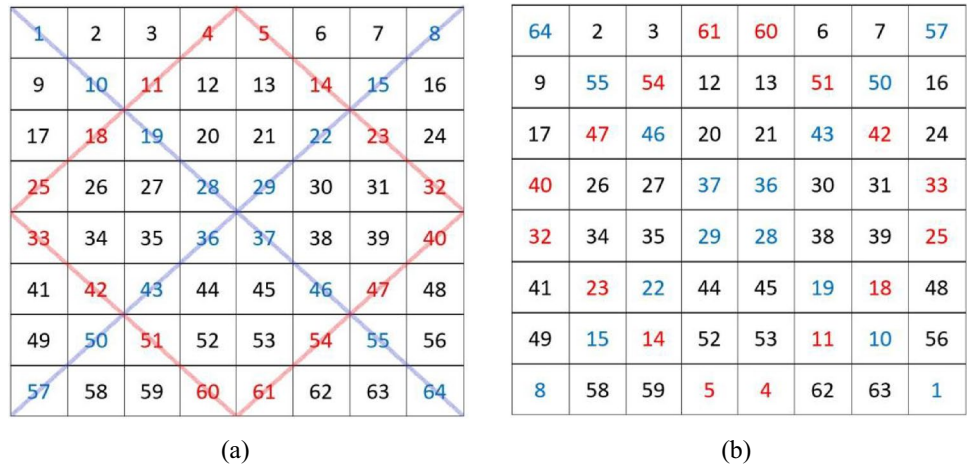
	2	3	4	5	6	7	8
9	10	11	12	13	14	15	16
17	18	19	20	21	22	23	24
25	26	27	28	29	30	31	32
33	34	35	36	37	38	39	40
41	42	43	44	45	46	47	48
49	50	51	52	53	54	55	56
57	58	59	60	61	62	63	64

(a)

1	48	31	50	33	16	63	18
30	51	46	3	62	19	14	35
47	2	49	32	15	34	17	
52	29	4	45	20	61	36	13
5	44	25	56	9	40	21	60
28	53	8	41	24	57	12	37
43	6	55	26	39	10	59	22
54	27	42	7	58	23	38	11

(b)

Fig. 4 (a) An 8×8 matrix numbered from 1 to 64 (b) Obtained Doubly Even-order Magic square matrix



Step 4: Then, extract these blue-coloured and red-coloured numbers from the 8×8 square and form them in a sequence as follows: 1–4–5–8–10–11–14–15–18–19–22–23–25–28–29–32–33–36–37–40–42–43–46–47–50–51–54–55–57–60–61–64.

Step 5: Fill up the empty cells (formed due to the extraction of coloured numbers in step 4) sequentially by reversing the order of the above-formed sequence as follows: 64–61–60–57–55–54–51--50–47–46–43–42–40–37–36–33–32–29–28–25–23–22–19–18–15–14–11–10–8–5–4–1.

The flowchart of detailed step by step procedure of the proposed KTM and DEM approaches is shown in Fig. 5(a) and (b) respectively.

Application of the Proposed Strategies in Reconfiguration

By using the proposed algorithms achieves uniform shade dispersion for irradiation equalisation, in contrast to the majority of existing reconfiguration solutions that distribute the shadow effect unevenly. In contrast to the current methodologies, this ensures reliable and optimal performance under any kind of shading environment. While the solar PV array is rearranged in accordance with a preconfigured rearranged matrix design pattern developed by using proposed algorithms. This ensures that the shading effect is significantly reduced but the electrical characteristics of the array are retained. The solar panels of the conventional TCT-configured array are realigned electrically or moved physically (as depicted in Fig.7) following the patterns of rearranged matrices obtained by the proposed strategies shown in Fig. 6. The obtained KTM matrix by the knight tour approach is applied for reconfiguration of the conventional TCT-configured PV array. The differences in architectural topological structure between TCT and the proposed KTM configuration is shown in Fig.7.

The Fig.7 shows the TCT-based configuration of the PV array where the panel number “27” is positioned in the fifth

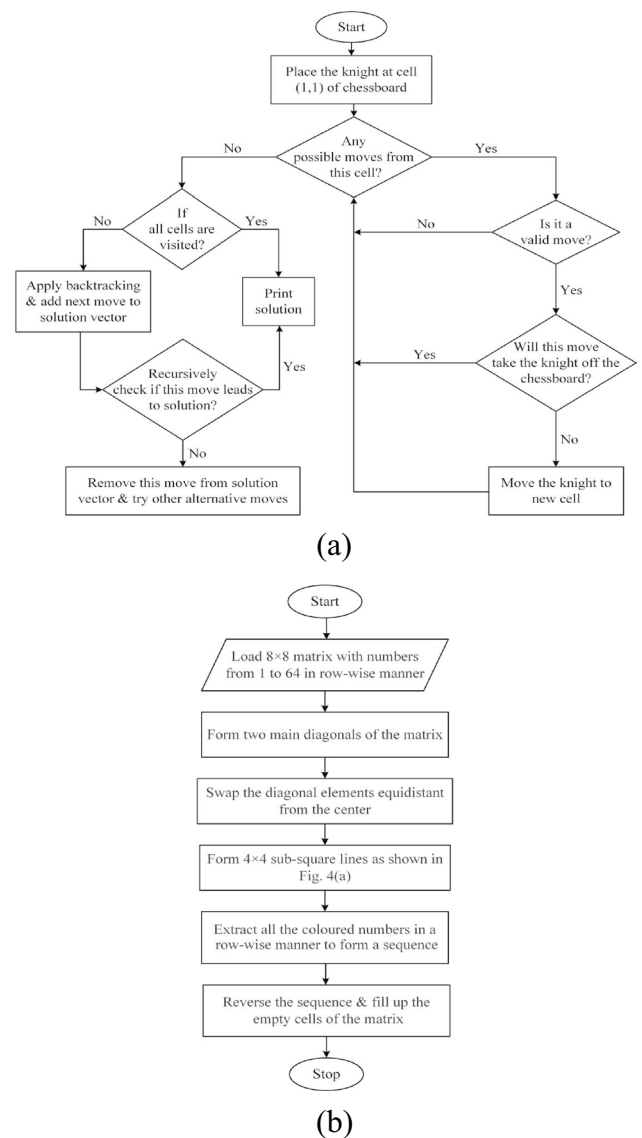


Fig. 5 Flowchart of detailed step by step procedure of (a) KTM and (b) DEM approaches

Fig. 6 Original and rearranged matrices obtained by KTM and DEM approaches

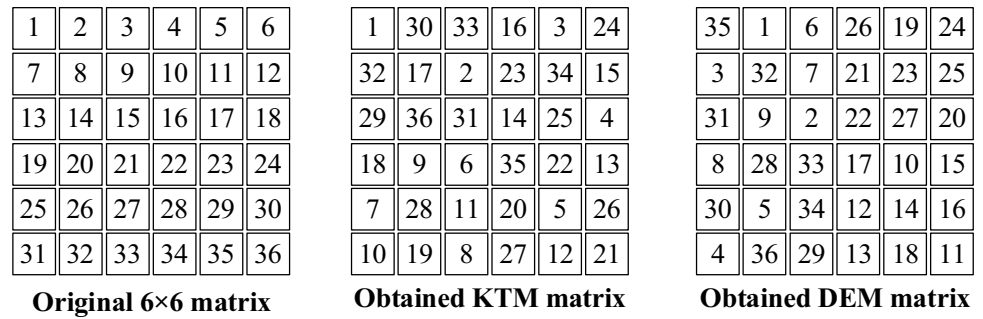


Fig. 7 (a) Conventional TCT and (b) proposed KTM configuration

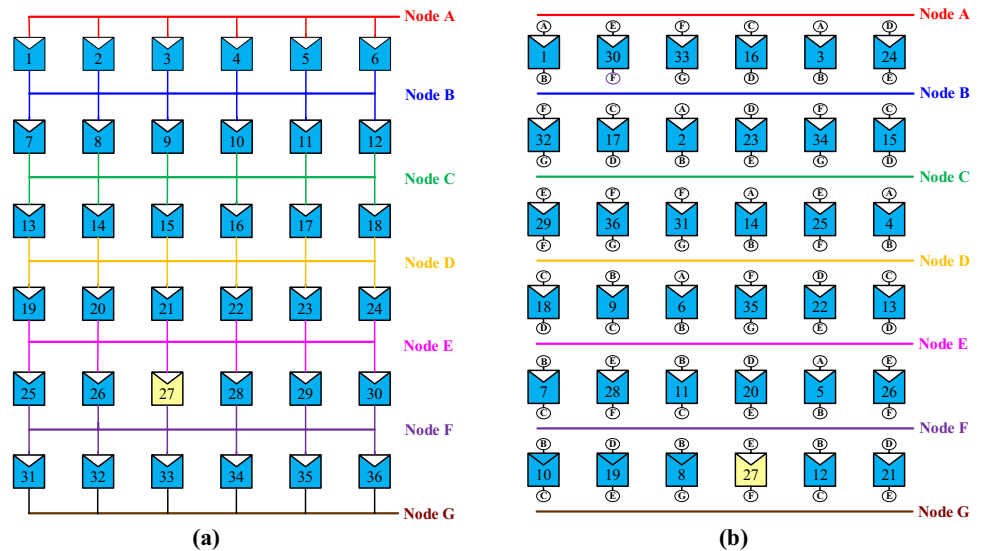
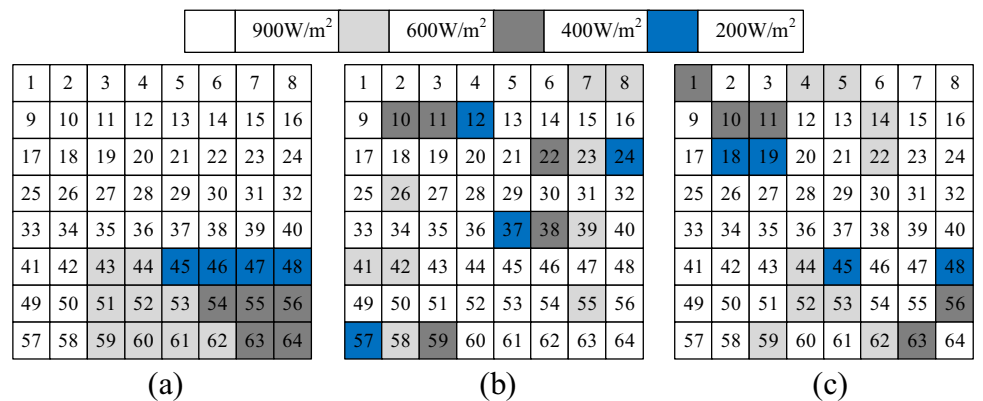


Fig. 8 Short-Broad shading pattern: (a) TCT configuration, shade dispersion with (b) KTM and (c) DEM techniques respectively



row and third column (between Node-E and Node-F). However, based on the rearranged matrices that were acquired, this panel is now oriented in the sixth row and the fourth column, as shown in Fig. 7. (b). Similar to this, all panels are effectively reconfigured using the rearranged matrices to disperse the shadow equitably. As an illustration, if the PV

panels (PV1, PV30, PV33, PV16, PV3, PV24) within the first row of the newly configured array are shadowed, this row-wise shadow effect is spread to all rows, maintaining the balanced irradiation throughout the rows and minimising the mismatch since these panels are positioned physically in the first row but are electrically connected to multiple rows.

Various Performance Parameters

To verify the effectiveness of the array configurations, the system is tested with the following performance parameters.

Mismatch Power (MM_p)

In a PV array, mismatch losses occur due to the interconnection of PV cells having different characteristics [38, 39] and it is the variation between GMP obtained under unshaded (GMP_{unshaded}) and shaded conditions (GMP_{shaded}).

$$MM_p(W) = GMP_{unshaded} - GMP_{shaded}$$

Percentage Power Loss (P_L)

It is the ratio of difference between GMP obtained at unshaded and shaded conditions to the GMP obtained under unshaded conditions.

$$P_L(\%) = \frac{GMP_{unshaded} - GMP_{shaded}}{GMP_{unshaded}}$$

Efficiency (η)

It is the ratio of PV array energy output to the amount of incident solar irradiation delivered by the sun. It is computed as follows:

$$\eta(\%) = \frac{V_{mpp} \times I_{mpp}}{G \times A}$$

where, ‘G’ is amount of solar irradiation (W/m²) and A is PV panel area (A = 1425 mm × 990 mm considered for analysis).

Performance Ratio (PR)

It is the ratio of GMP obtained under PS conditions to the GMP obtained under standard test conditions (STC). PR gives what factor of the generated solar energy is utilized efficiently.

$$PR(\%) = \frac{GMP_{PS}}{GMP_{STC}}$$

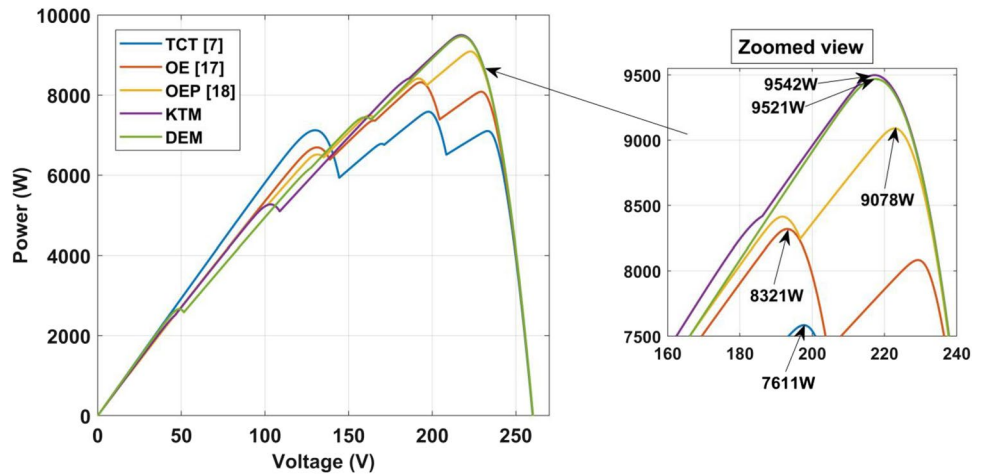
Results and Discussion

To attain effective shade dispersal, the PV array is reconfigured by using the rearranged matrices obtained by KTM and DEM approaches as shown in Figs. 3(b) and 4(b) respectively. Further, to substantiate the effectiveness of both the proposed techniques over the notable benchmark TCT configuration and

Table 1 Comparison of theoretical computations of TCT, KTM and DEM configurations under SB pattern

TCT Configuration				KTM Configuration				DEM Configuration			
Row No.	Current I _{rk} (A)	Voltage V _m (V)	Power P _m (W)	Row No.	Current I _{rk} (A)	Voltage V _m (V)	Power P _m (W)	Row No.	Current I _{rk} (A)	Voltage V _m (V)	Power P _m (W)
R ₆	3.8I _m	8V _m	30.4V _m I _m	R ₂	5.5I _m	8V _m	44V _m I _m	R ₃	5.5I _m	8V _m	44V _m I _m
R ₇	4.8I _m	7V _m	33.6V _m I _m	R ₃	5.7I _m	7V _m	39.9V _m I _m	R ₆	-	8V _m	-
R ₈	5.0I _m	6V _m	30V _m I _m	R ₅	-	-	-	R ₂	5.9I _m	6V _m	35.4V _m I _m
R ₁	7.2I _m	5V _m	36V _m I _m	R ₈	-	-	-	R ₁	6.1I _m	5V _m	30.5V _m I _m
R ₂	-	-	-	R ₁	6.6I _m	4V _m	26.4V _m I _m	R ₇	-	-	-
R ₃	-	-	-	R ₆	-	-	-	R ₈	-	-	-
R ₄	-	-	-	R ₄	6.9I _m	2V _m	13.8V _m I _m	R ₄	7.2I _m	2V _m	14.4V _m I _m
R ₅	-	-	-	R ₇	-	-	-	R ₅	-	-	-

Fig. 9 Power-Voltage characteristics of TCT, KTM and DEM under SB shading pattern



the existing odd-even (OE) and odd-even-prime (OEP) strategies, an 8×8 PV array configured in TCT [7], OE [17], OEP [18], KTM and DEM arrangements has been tested using MATLAB software. The efficacy of the proposed techniques is tested under four non-uniform and uniform-shading patterns with the aforementioned five performance indices. The performance parameter values of various array configurations under different shading conditions are given in Fig. 22 and Table. 4. The performance investigation under various shading conditions is performed as follows: The GMP obtained by TCT configuration under STC is 11,582.1 W.

During the non-uniform shading conditions, all the unshaded modules are considered to receive irradiation of 900 W/m^2 whereas shaded modules receive the irradiation of 600 W/m^2 , 400 W/m^2 , and 200 W/m^2 .

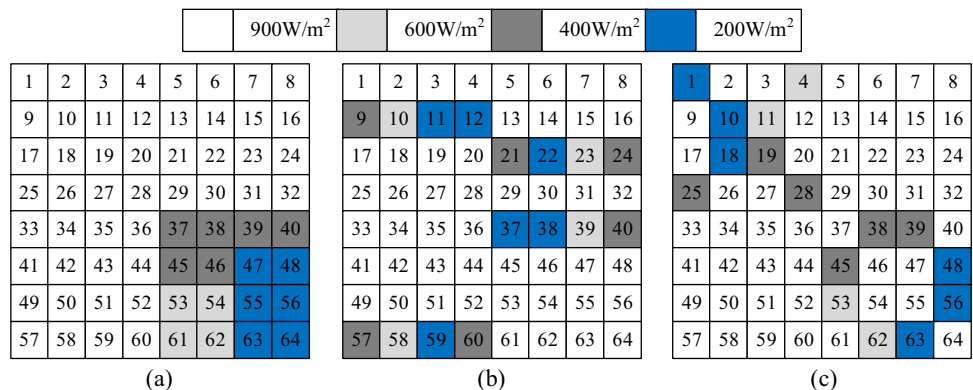
Under Short-Broad (SB) Type Shading

During SB shading, the shading pattern considered is short and broad typed as shown in Fig. 8(a) and the shade dispersion with KTM and DEM techniques are shown in Figs. 8(b) and 8(c) respectively.

In an array, the number of variations in the row currents indicates the number of bypasses. Table 1 gives the comparative analysis of theoretical computations of various configurations under SB pattern. It is noted that for TCT configuration, the row currents vary from 3.8 Im to 7.2 Im and this large variation is significantly reduced by employing KTM and DEM techniques which vary from 5.7 Im to 6.9 Im and 5.5 Im to 7.2 Im respectively. This is clearly manifested in the significant enhancement in power-voltage characteristics as shown in Fig. 9 which has very fewer multiple peaks and is closer to the ideal characteristics. Both the proposed KTM and DEM techniques generate the highest GMP of 44 VmIm compared to TCT which is only 36 VmIm . The improved power-voltage (PV) and current-voltage (IV) characteristics obtained by the proposed KTM, and DEM facilitates the efficient tracking of the global maximum power. Further, due to the mitigated row current mismatch through shade dispersion by the KTM and DEM approaches, the global maximum power has been augmented significantly.

The GMP obtained by TCT configuration is 7611 W. The concentrated SB shading has been effectively dispersed by KTM technique which yields the GMP of 9521 W which

Fig. 10 Short-Narrow shading pattern: (a) TCT configuration, shade dispersion with (b) KTM and (c) DEM techniques respectively



is 25.1% more than TCT. Similarly, DEM technique also yields the highest GMP of 9542 W which is 25.4% more than TCT. Further, the existing OE and OEP configurations despite scalable for all array sizes, fail to disperse the shade uniformly thereby yielding more mismatch losses. The GMP obtained by OE and OEP arrangements are 8321 W and 9078 W which is only 9.32% and 19.27% respectively. The respective MM_p obtained by the proposed KTM, and DEM configurations is also reduced significantly. It is noted that the proposed techniques reduce MM_p nearly by 50% compared to conventional TCT.

The respective P_L computed for KTM, and DEM techniques is 17.79% and 17.61% that again confirms that the proposed techniques are preferable over conventional ones. The KTM and DEM techniques have the maximum generated efficiency of 13.6% and 13.63% respectively when compared with TCT which is only 10.87%. It is remarkably manifested in the fact that the values of PR, and MM_p are more superior to conventional TCT.

Under Short-Narrow (SN) Type Shading

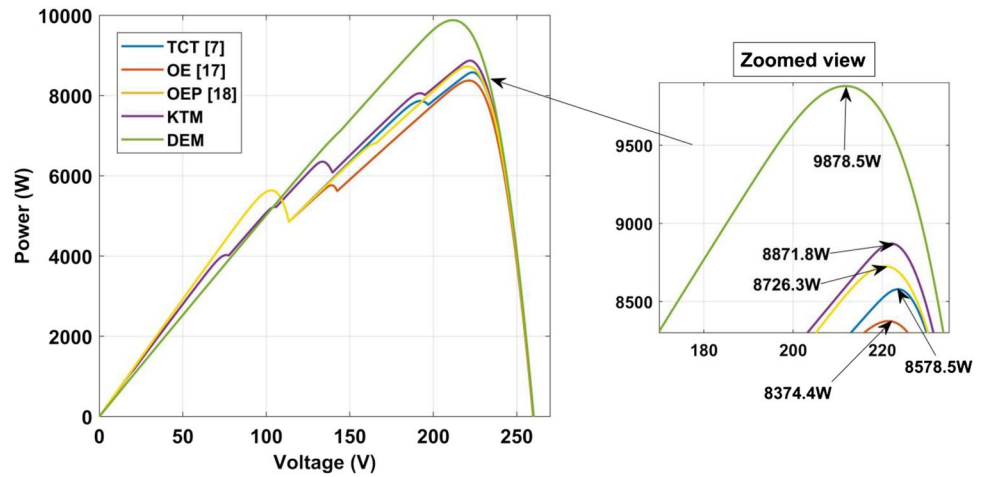
The shading pattern considered is short and narrow in which the lower right part of the array has been shaded as shown in Fig. 10(a) and the shade dispersion with KTM and DEM techniques - are shown in Figs. 10(b) and 10(c) respectively. The theoretical computations for TCT, KTM, and DEM techniques explicates that DEM technique yields the lowest row current variation with only two bypasses as shown in Table 2 and thus providing much smoother power-voltage characteristics as shown in Fig. 11. By employing the DEM technique, a very narrow range of row current variations is achieved i.e., from 6Im to 6.2Im. Followed by DEM, the KTM technique also provides smoother characteristics compared to TCT. The GMP obtained by DEM and KTM techniques are 48VmIm and 40VmIm which is highest compared to TCT which yields only 38.4VmIm.

Under, this condition, the GMP obtained by TCT, KTM and DEM techniques is 8578.5 W, 8871.8 W, 9878.5 W respectively. The respective DEM and KTM techniques distribute the shade effectively thereby enhancing the GMP by 1300 W and 293.3 W which is 15.16% and 3.42% more than TCT. During this case, the existing odd-even strategy yields very lower power (-2.4%) even compared to the standard benchmark TCT configuration. Besides, the improved OE strategy named as odd-even-prime strategy also underperforms in this case maximizing the GMP only by 1.72%. The MM_p obtained by TCT, KTM, and DEM configuration is 3003.5 W, 2710.2 W, and 1703.5 W. The proposed DEM and KTM techniques reduce the MM_p by significant percentage when compared to TCT. The P_L computed for TCT is 25.93%, whereas the respective DEM and KTM techniques reduce it to 14.7% and 23.4%. The DEM technique yields

Table 2 Comparison of theoretical computations of TCT, KTM and DEM configurations under SN pattern

TCT Configuration				KTM Configuration				DEM Configuration			
Row No.	Current I_{Ri} (A)	Voltage V_m (V)	Power P_m (W)	Row No.	Current I_{Ri} (A)	Voltage V_m (V)	Power P_m (W)	Row No.	Current I_{Ri} (A)	Voltage V_m (V)	Power P_m (W)
R ₆	4.8I _m	8V _m	38.4V _m I _m	R ₂	5.0I _m	8V _m	40V _m I _m	R ₃	6.0I _m	8V _m	48V _m I _m
R ₅	5.2I _m	7V _m	36.4V _m I _m	R ₅	-	-	-	R ₆	-	-	-
R ₇	-	-	-	R ₃	5.2I _m	6V _m	31.2V _m I _m	R ₁	6.2I _m	6V _m	37.2V _m I _m
R ₈	-	-	-	R ₈	-	-	-	R ₂	-	-	-
R ₁	7.2I _m	4V _m	28.8V _m I _m	R ₁	7.2I _m	4V _m	28.8V _m I _m	R ₄	-	-	-
R ₂	-	-	-	R ₄	-	-	-	R ₅	-	-	-
R ₃	-	-	-	R ₆	-	-	-	R ₇	-	-	-
R ₄	-	-	-	R ₇	-	-	-	R ₈	-	-	-

Fig. 11 Power-Voltage characteristics of TCT, KTM and DEM under SN shading pattern



the highest efficiency, which is 14.23%. Followed by KTM (12.78%) and TCT (12.35%) configurations. The efficacy of the respective DEM and KTM techniques is evinced with a greater PR of 0.852 and 0.765. Further, both DEM and KTM techniques provides an extremely better performance which is also manifested in the enhancement of the array characteristics.

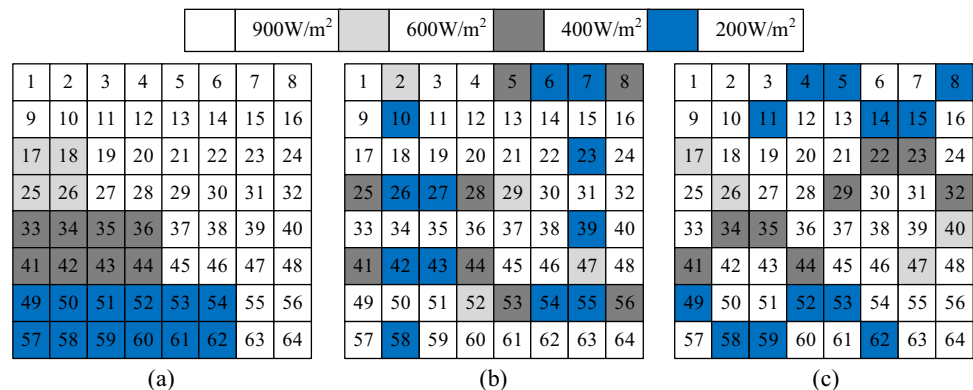
Under Long-Broad (LB) Type Shading

The shading pattern considered is long and broad typed as shown in Fig. 12(a) and the shade dispersion with KTM and DEM techniques are shown in Figs. 12(b) and 12(c) respectively. The maximum power output obtained by TCT, KTM, and DEM techniques is 31.2VmIm, 36VmIm, and 40.8VmIm. It is noticed that from Table. 3 that by employing the DEM and KTM techniques, a narrow range of row current variation is obtained which is from 5.2Im to 6.6Im and 5.1Im to 7.2Im respectively. This narrow range has led to the reduction of multiple peaks thereby obtaining smooth characteristics of an array as shown in Fig. 13. However, the conventional TCT yields a comparatively broad range of row currents varying from 4.5Im

to 7.2Im, thus exhibiting many bypasses. The number of bypasses obtained by TCT is four and these bypasses are significantly reduced by half by employing the proposed KTM and DEM techniques. By executing the proposed approaches, the smoother characteristics are obtained exhibiting only one global and local power peak, whereas the conventional TCT exhibits four multiple power peaks. This causes the misleading of tracking the global maximum power from the conventional TCT array configuration and the MPPT controllers stuck at a local optimum extracting sub-optimal output from the array.

The conventional TCT generates the GMP of 6770.4 W whereas the proposed DEM configuration yields 8559.6 W which is 26.43% more than TCT. The proposed KTM technique also yields 15.97% more than TCT configuration which is 1080.74 W. The MATLAB computational results show that the proposed DEM and KTM techniques yield superior performance with the reduced mismatch power of 7623 W and 9683 W respectively which is 36.59% and 19.45% less when compared to TCT (12,021 W). Following the proposed strategies, the existing OE and OEP configurations yield the enhancement of only 6870.7 W and 7752.4 W which is 1.48% and 14.5% more respectively.

Fig. 12 Long-Broad shading pattern: (a) TCT configuration, shade dispersion with (b) KTM and (c) DEM techniques respectively



It is observed that the proposed DEM technique holds the first leading place giving the reduced P_L of 26.09%, efficiency of 11.29%. Furthermore, this technique gives a peerless performance with a PR of 0.739. Followed by DEM, the KTM technique holds the next leading place by proffering the reduced P_L of 32.21%, efficiency of 10.37%. Besides these factors, this technique also yields better performance with a PR of 0.677.

To further, demonstrate the employability of the proposed techniques, various cases of following uniform shading patterns are also considered. Here, the un-shaded and shaded modules are considered to receive irradiation of 900 W/m² and 500 W/m² respectively.

Under L-Shaped Shading

In this condition, the pattern of the shading is L-shaped as shown in Fig. 14(a) and the shade dispersion with KTM and DEM techniques are shown in Figs. 14(b) and 14(c) respectively. During this condition, TCT yields the GMP of 9200 W whereas the proposed KTM technique yields the GMP of 9808 W which is 608 W (6.06%) more than the TCT configuration. The DEM configuration yields the GMP of 10,175 W which is 975 W (10.61%) more than that of TCT. The proposed DEM technique yields extremely superior performance over TCT by yielding the reduced MM_p of 1407 W, P_L of 12.14%, efficiency of 14.09%, and PR of 0878. The proposed DEM and -KTM techniques yield smoother array power-voltage characteristics compared to TCT configurations which is shown in Fig. 15.

Under Triangle-Shaped Shading

Here, the lower triangular part of the 8×8 PV array is shaded as shown in Fig. 16(a) and the shade dispersion with KTM and DEM techniques are shown in Figs. 16(b) and 16(c) respectively. The concentrated shading subjected over the corner portion of the PV array is dispersed into various rows of the array through the KTM and DEM configurations. The conventional TCT array configuration exhibits five bypasses (five power peaks) in the array characteristics. Whereas the proposed strategies mitigate these peaks to a significant extent as shown in the Fig. 16 of power-voltage characteristics of the array. The respective DEM and KTM techniques yield the GMP of 10,659 W and 10,343 W which is 7.19% and 4.02% than TCT.

The proposed DEM and KTM techniques performed better than TCT in delivering outstanding performance with additional parameters like MM_p , P_L , efficiency, and PR. The respective values obtained with KTM configurations are 1239 W, 10.69%, 13.67%, and 0.893 respectively

Table 3 Comparison of theoretical computations of TCT, KTM and DEM configurations under LB pattern

TCT Configuration				KTM Configuration				DEM Configuration			
Row No.	Current I_{Ri} (A)	Voltage V_m (V)	Power P_m (W)	Row No.	Current I_{Ri} (A)	Voltage V_m (V)	Power P_m (W)	Row No.	Current I_{Ri} (A)	Voltage V_m (V)	Power P_m (W)
R ₇	3.0 I_m	8 V_m	24 $V_m I_m$	R ₁	4.5 I_m	8 V_m	36 $V_m I_m$	R ₁	5.1 I_m	8 V_m	40.8 $V_m I_m$
R ₈	3.0 I_m	-	-	R ₄	-	-	-	R ₂	-	-	-
R ₅	5.2 I_m	6 V_m	31.2 $V_m I_m$	R ₆	-	-	-	R ₇	-	-	-
R ₆	5.2 I_m	-	-	R ₇	-	-	-	R ₈	-	-	-
R ₃	6.6 I_m	4 V_m	26.4 $V_m I_m$	R ₂	6.5 I_m	4 V_m	26 $V_m I_m$	R ₃	5.9 I_m	4 V_m	23.6 $V_m I_m$
R ₄	6.6 I_m	-	-	R ₃	-	-	-	R ₄	-	-	-
R ₁	7.2 I_m	2 V_m	14.4 $V_m I_m$	R ₅	-	-	-	R ₅	-	-	-
R ₂	7.2 I_m	-	-	R ₈	-	-	-	R ₆	-	-	-

Fig. 13 Power-Voltage characteristics of TCT, KTM and DEM under LB shading pattern

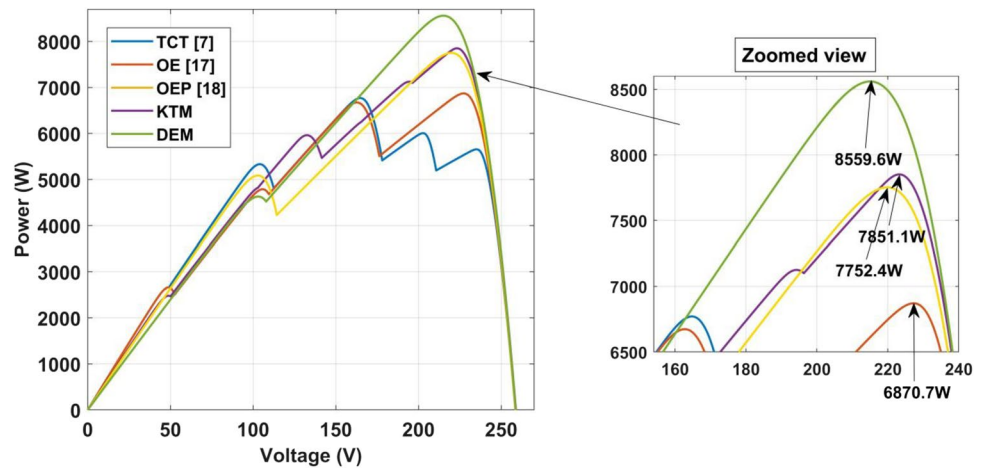


Fig. 14 L-shaped shading pattern: (a) TCT configuration, shade dispersion with (b) KTM and (c) DEM techniques respectively

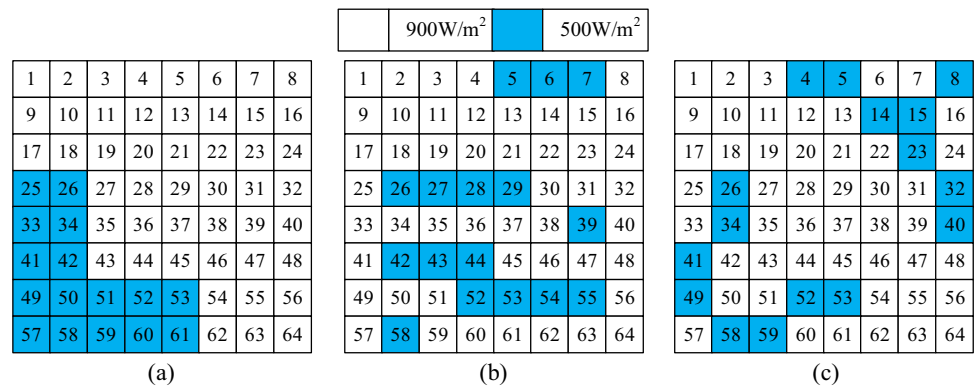


Fig. 15 Power-Voltage characteristics of TCT, KTM and DEM under L-shaped pattern

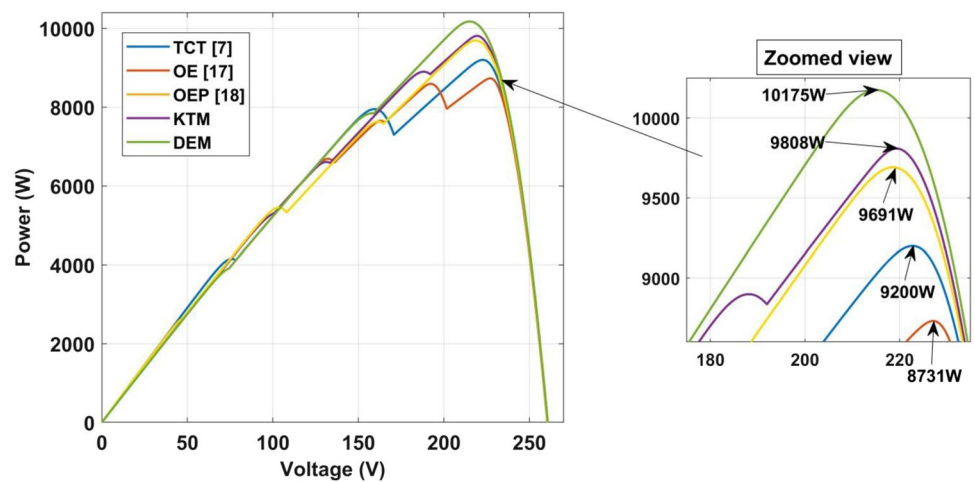


Fig. 16 Triangle-shaped shading pattern: (a) TCT configuration, shade dispersion with (b) KTM and (c) DEM techniques respectively

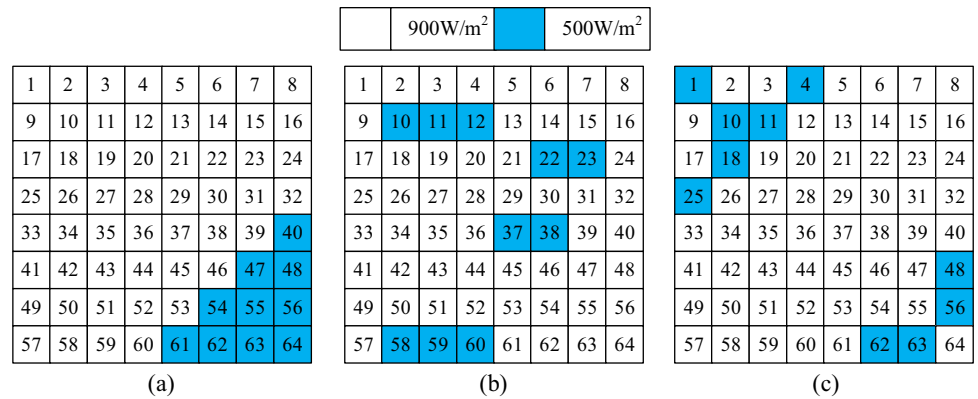


Fig. 17 Power-Voltage characteristics of TCT, KTM and DEM under triangle-shaped pattern

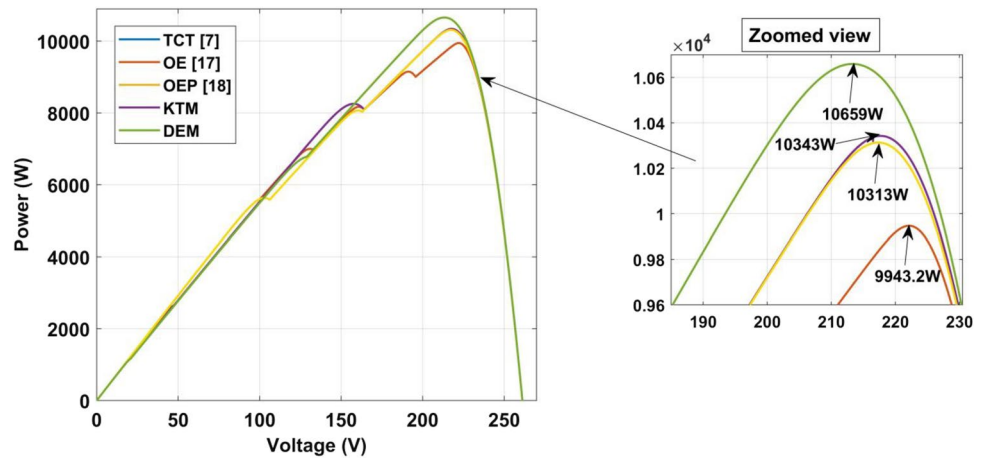


Fig. 18 Rhombus-shaped shading pattern: (a) TCT configuration, shade dispersion with (b) KTM and (c) DEM techniques respectively

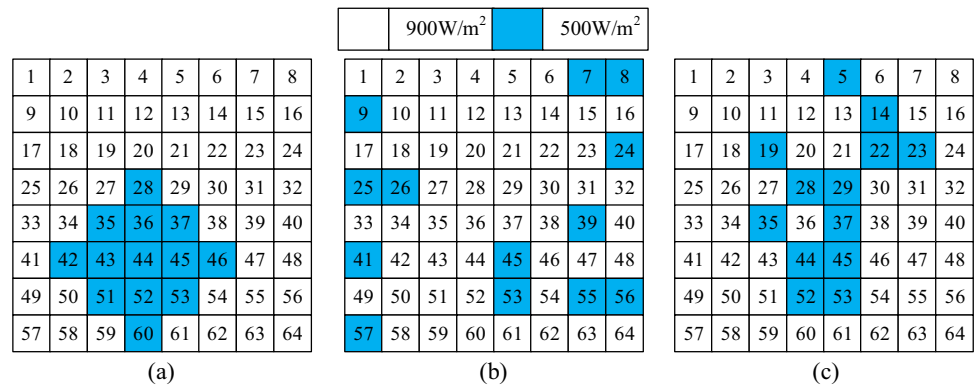


Fig. 19 Power-Voltage characteristics of TCT, KTM and DEM under rhombus-shaped pattern

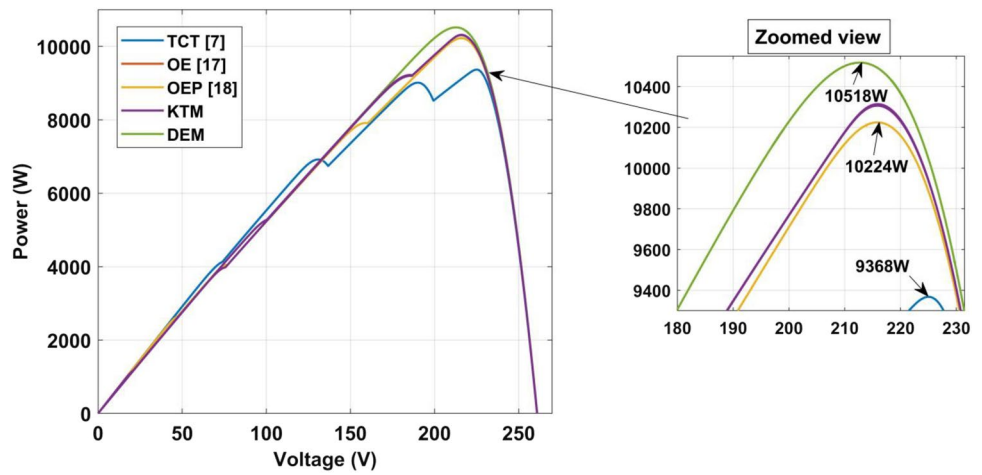


Fig. 20 Square-shaped shading pattern: (a) TCT configuration, shade dispersion with (b) KTM and (c) DEM techniques respectively

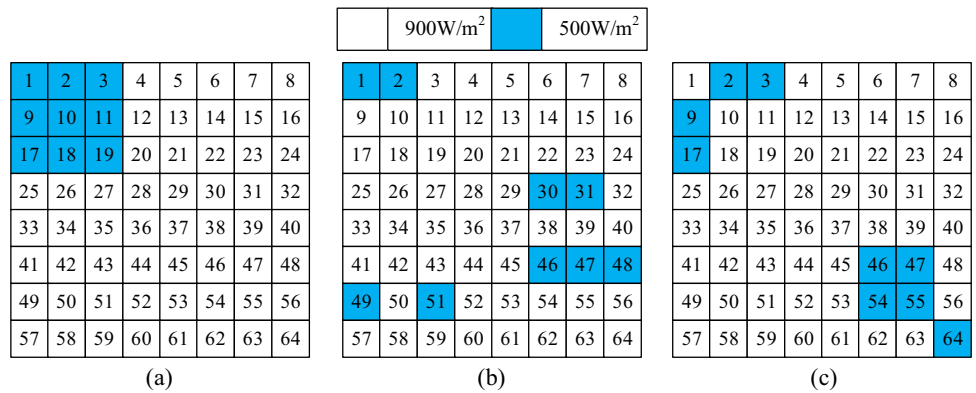


Fig. 21 Power-Voltage characteristics of TCT, KTM and DEM under square-shaped pattern

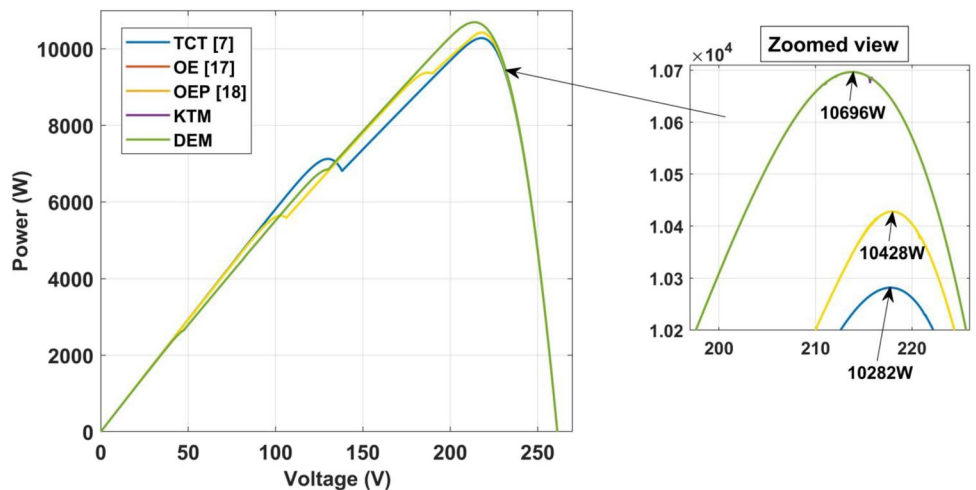


Table 4 Comparison of GMP enhancement, mismatch power, and performance ratio under various non-uniform PS patterns

Configura- tion	% GMP more w.r.t TCT	MM _p (W)	P _L (%)	Efficiency (%)	P.R
Under Short-Broad shading condition:					
TCT [7]	–	3971	34.28	10.87	0.657
OE [17]	9.32	3261	28.15	11.89	0.718
OEP [18]	19.27	2504	21.61	12.97	0.783
KTM	25.09	2061	17.79	13.60	0.822
DEM	25.38	2040	17.61	13.63	0.823
Under Short-Narrow shading condition:					
TCT [7]	–	3003.5	25.93	12.35	0.740
OE [17]	–2.37	3207.6	27.69	12.06	0.723
OEP [18]	1.72	2855.7	24.65	12.57	0.753
KTM	3.41	2710.2	23.40	12.78	0.765
DEM	15.16	1703.5	14.70	14.23	0.852
Under Long-Broad shading condition:					
TCT [7]	–	4811.6	41.54	8.93	0.584
OE [17]	1.48	4711.3	40.67	9.069	0.593
OEP [18]	14.50	3829.6	33.06	10.23	0.669
KTM	15.96	3730.9	32.21	10.37	0.677
DEM	26.43	3022.4	26.09	11.29	0.739
Under L-shaped shading condition:					
TCT [7]	–	2382	20.56	12.73	0.794
OE [17]	–5.09	2851	24.61	12.08	0.753
OEP [18]	5.33	1891	16.32	13.41	0.836
KTM	6.60	1774	15.31	13.58	0.846
DEM	10.61	1407	12.14	14.09	0.878
Under Triangle-shaped shading condition:					
TCT [7]	–	1638.8	14.14	13.14	0.858
OE [17]	0	1638.8	14.14	13.14	0.858
OEP [18]	3.71	1269	10.95	13.63	0.890
KTM	4.02	1239	10.69	13.67	0.893
DEM	7.19	923	7.96	14.09	0.920
Under Rhombus-shaped shading condition:					
TCT [7]	–	2214	19.11	11.54	0.808
OE [17]	12.27	1064	9.18	12.96	0.908
OEP [18]	9.13	1358	11.72	12.60	0.882
KTM	10.09	1268	10.94	12.72	0.890
DEM	10.02	1276	11.01	12.72	0.889
Under Square-shaped shading condition:					
TCT [7]	–	1300	11.22	13.49	0.887
OE [17]	0	1300	11.22	13.49	0.887
OEP [18]	1.41	1154	9.96	13.68	0.900
KTM	4.02	886	7.64	14.05	0.923
DEM	4.03	886	7.64	14.05	0.923

whereas the respective values obtained with DEM technique are 923 W, 10.69%, 14.09%, and 0.920 respectively. When compared to TCT, the array characteristics are improved by employing proposed techniques as shown in Fig. 17

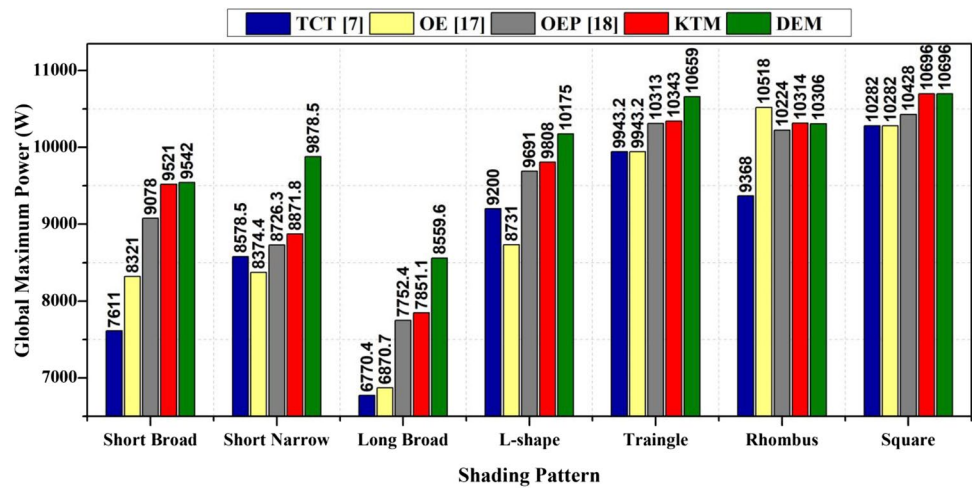
Under Rhombus-Shaped Shading

A special shading pattern in the form of a rhombus has been considered as shown in Fig. 18(a) and the shade dispersion with KTM and DEM techniques are shown in Figs. 20(b) and 20(c) respectively. The concentrated shadow covering the significant portion of the PV array leads to the mismatch between the distinct rows of the array. Due to the mismatch, the irradiation levels in all the rows are unbalanced by a considerable amount. Further, this concentrated shade has been dispersed to various rows mitigating the mismatch and improving the array characteristics. The TCT configuration generates the GMP of 9368 W. The proposed KTM and DEM configuration yields the GMP of 10,338 W and 10,518 W which is 990 W (10.35%) and 1150 W (12.27%) more compared to the TCT configuration. The performance of the DEM technique is on par with the KTM technique under this shading condition. The proposed KTM technique yields the lowest MM_p, lowest P_L, highest efficiency, and highest PR with the values of 1239 W, 10.69%, 13.67%, and 0.893 respectively. The respective power-voltage characteristics are shown in Fig. 19.

Under Square-Shaped Shading

The small portion of the PV array is considered to be subjected to a square-shaped shading pattern at the upper left corner of the array as shown in Fig. 20(a). The shade dispersion with the KTM and DEM techniques are shown in Figs. 20(b) and 20(c) respectively. The GMP obtained for TCT, KTM and DEM configurations are 10,282 W, 10,696 W, and 10,696 W respectively. By employing the DEM and KTM techniques, the respective enhancement in GMP is 4.02% and 4.03% compared to that of the conventional TCT configuration. The proposed DEM technique yields the lowest MM_p, lowest % power loss, highest efficiency, and highest PR with the values of 886 W, 7.64%, 14.05%, and 0.923 respectively. The respective power-voltage characteristics are shown in Fig. 20. It is observed from the figure that the array PV characteristics (Fig. 21)

Fig. 22 Comparison of global maximum power under various non-uniform and uniform shading conditions



are enhanced significantly due to the mitigation of row-current mismatch in the KTM and DEM configurations of the PV array. The power enhancement after the reconfiguration is less which is approximately 4% since the shaded area of the PV array is less. Besides, both the proposed configurations effectively disperse the shade over the array to mitigate the losses.

A comparison of the global maximum power of PV array configured in various configurations has been shown in

Table 4. Further, the other additional performance parameters such as mismatch power, and PR under various PS patterns are given in Table 4 respectively. It is noted from Fig. 22 that the proposed configurations offer superior and consistent performance under all the shading conditions. Further, when compared to the KTM approach, the DEM configuration exhibited superior performance due to its lowest correlation between the adjoining panels of the reconfigured array Fig. 23.

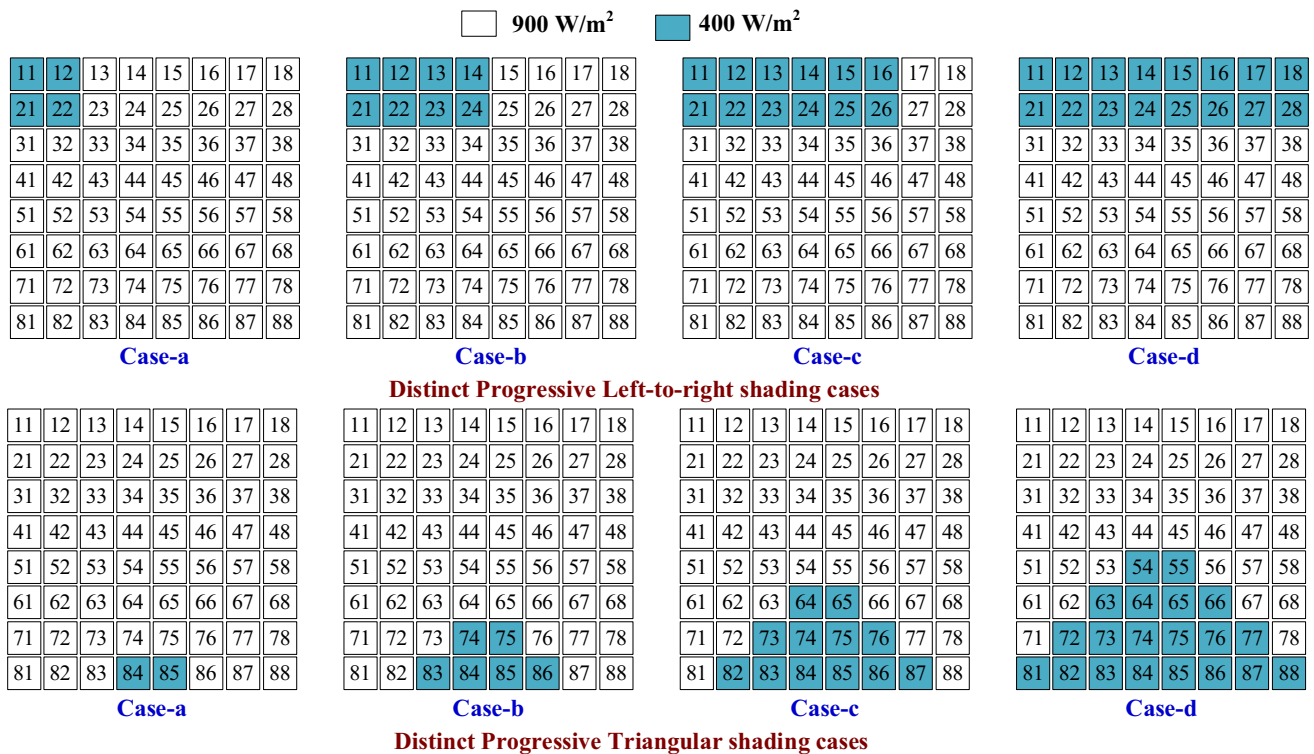


Fig. 23 Various progressive dynamic shading cases considered for analysis

Table 5 Comparison of GMP for various configurations under progressive shading conditions

Global Maximum Power (in Watt)			
Progressive Left-to-right Shading	Configuration	KTM	DEM
	Case-a	1070.1	11,071
Case-b	9283.0	10,416	10,416
Case-c	8609.2	9787.0	10,265
Case-d	8609.1	9024.6	9984.5
Progressive Triangular Shading	Configuration	KTM	DEM
	Case-a	10,884	10,884
Case-b	9463.4	10,267	11,258
Case-c	8211.8	9175.1	9493.6
Case-d	6967.2	8942.0	9113.8

The bold values indicate the highest values obtained for the proposed configurations

Under Distinct Progressive Shading Conditions

The proposed KTM and DEM configurations, the existing OE [17], the existing OEP [18], and the conventional TCT [7], are examined and tested under various shading scenarios of distinct shading groups, such as progressive left-to-right and triangular shading scenarios as shown in Fig. 5. The most common manifestations of these shadings include adjacent panel shading, high structures close by, moving clouds, raised poles, skyscrapers, chimneys, roof accessories, etc., whose density goes up over time. When held as independent shading cases, these shading cases have the advantage of acting as both dynamic and static shades. The system is evaluated using the global maximum power performance indicator to confirm the superiority of the recommended configurations.

The performance of the proposed configurations has been verified under static shading conditions as detailed in Section.6.1 to 6.8. Further, it is also noted from Table 5 that the proposed configurations also perform efficiently even under moving cloud/shade conditions. It is evident from the table that there exists a significant difference between the GMP obtained by the proposed and the conventional TCT configuration

Validation of Proposed Approaches for Asymmetrical PV Arrays

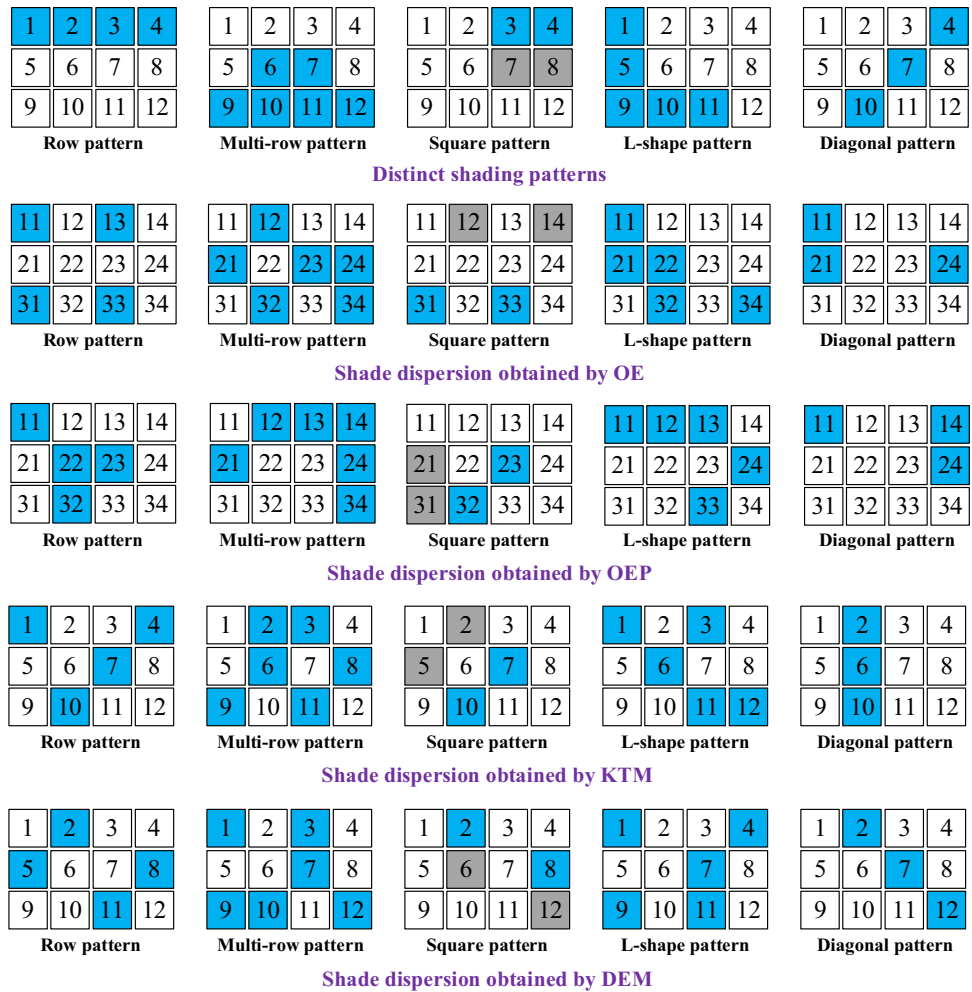
In the practical real-time scenario, the PV arrays could be symmetric or asymmetrical. Numerous static reconfiguration methods [14–16, 19–29] mentioned in the literature cannot be used for the asymmetrically sized PV arrays such as 4×5 , 7×9 , 11×8 , etc. Consequently, their range of applications is very limited for employment. Whereas, the conventional array configurations, despite being scalable for all array sizes, have zero shadow dispersion ability and cannot reduce the mismatch between the rows of an array. So, very recently, two methodologies based on the odd-even (OE) and odd-even-prime (OEP) patterns are reported to overcome the scalability issues for the asymmetrical arrays. Nevertheless, as mentioned and proved in [4], that the existing OE and OEP approaches, despite being adaptable to any array size, have very poor shade dispersal capability because of their inefficient reconfiguration process involved.

To verify the scalability and compatibility of the proposed techniques for asymmetrical PV array sizing, a 3×4 PV array is considered for the analysis. Additionally, to demonstrate the effectiveness of the proposed configurations, their results have been compared with that of the recently reported OE and OEP-based strategies under various shading conditions shown in Fig. 24. It is evident from the figure that the proposed strategies distribute the shade effectively and uniformly over the array when compared to the existing OE and OEP strategies. Besides, it is also clearly observed from the array characteristics as shown in Fig. 25, that the proposed strategies yield the highest GMP compared to the OE, OEP, and TCT configurations. Moreover, the proposed configurations exhibit comparatively better characteristics that are close to the ideal ones. Further, it is noted from Fig. 25 and Fig. 26, that the existing OE and OEP exhibits poor shade dispersion under the diagonal case yielding 10.31% lowered power even compared to the conventional TCT configuration. Hence, due to the highly inconsistent performance of the OE and OEP, the proposed strategies are preferred over them. The GMP

Table 6 GMP (in Watt) obtained for a 4×3 PV array under various shading patterns

Configuration	Row-pattern	Multi-row pattern	Square-pattern	L-shape pattern	Diagonal pattern
TCT	1428.4	1102.4	1445.6	1397.4	1872.1
OE	1637.7	1381.6	1445.6	1619.5	1697.2
OEP	1677.6	1385.3	1516.6	1397.4	1697.2
KTM	1680.2	1388.9	1559.4	1621.9	1872.1
DEM	1683.6	1572.7	1561.8	1624.3	1872.1

Fig. 24 Various shading cases and the corresponding shade dispersion obtained for various approaches



obtained by various configurations of the asymmetrical arrays are given in Table 6.

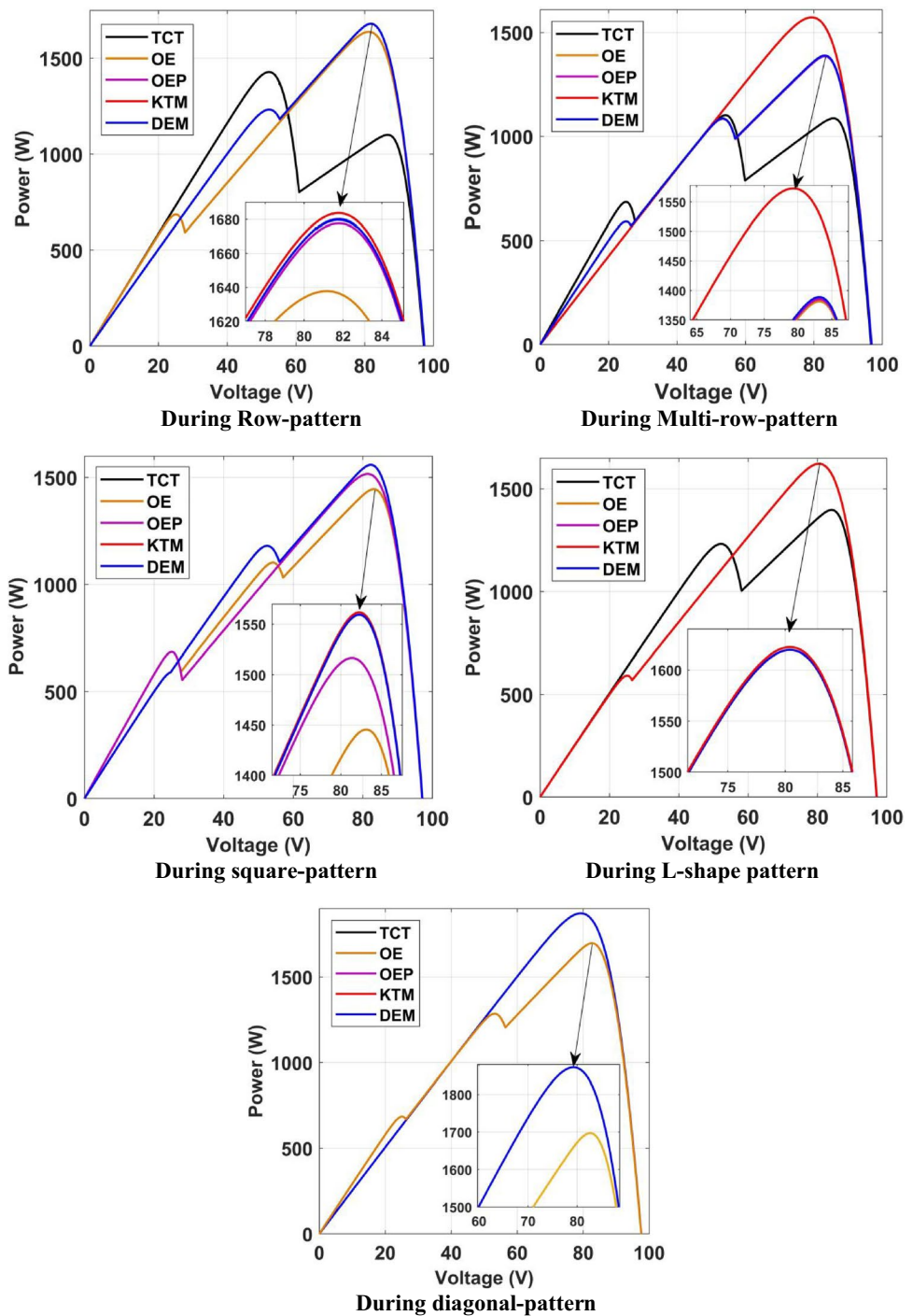
Economic Analysis

During unshaded conditions, the PV array generates 69.492 units/day. However, under various shadowing conditions, the output is limited as the mismatch losses are increased significantly [40]. These drawbacks can be reduced to the maximum extent by employing the proposed shadow dispensing techniques. To demonstrate the effectiveness, feasibility, and usefulness of the suggested techniques, the generated electricity units and the revenue growth are assessed and investigated. During the normal days, the PV array functions effectively during the peak sun hours, so for analysis, three aforementioned shading patterns (SB, SN and LB) are considered to take place over the array each hour from 10 a.m. to 4 p.m. The solar power tariff of ₹3 (INR) per unit is considered

for assessment. A comparative analysis of the respective units and revenue generated is shown in Figs. 27 and 28.

The units generated per day by TCT, KTM, and DEM techniques are 51.47kWh, 56.7kWh, and 59.12kWh respectively. The respective units generated per year 154.4kWh, 170.126kWh, and 177.361kWh. So, for a year, the proposed DEM and KTM techniques generates 1812.65 and 2795.9 units more compared to TCT configuration respectively. By employing the proposed DEM and KTM techniques, the respective revenue generation is increased by ₹5735.99 (INR) and ₹8379.31 (INR) which is 14.9% and 10.18% and more compared to the benchmark TCT. From the comparative economic analysis as given in Table 7, it is deserving to acknowledge that both proposed DEM and KTM techniques effectively disperses the shadow over the array and are best suitable to be employed under the partial shading conditions. By increasing the ratings of PV panels, the output power is maximized thereby maximizing the revenue generated.

Fig. 25 PV array characteristics obtained for unsymmetrical PV arrays under distinct cases



Comparison of the Proposed Approaches in Comparison to the State-of-the-Art Strategies

The advantages of the proposed approaches in comparison to the current state-of-the-art strategies are listed as follows:

- The proposed approaches do not use switching matrices, choose switching matrices at the best possible rate, and

furthermore do not have memory-related switching matrix operation problems, in contrast to AI approaches [5, 6].

- The EAR-based approaches [7, 8] demand for a controller to feed the switching pulses for the switches that correspond to the appropriate shade dispersion. In addition, a large number of switching patterns are required to determine the best PV array reconfiguration strategy. On the contrary, the suggested techniques eliminate the necessity of these operations.

Fig. 26 (a) Number of units generated per day and (b) per year

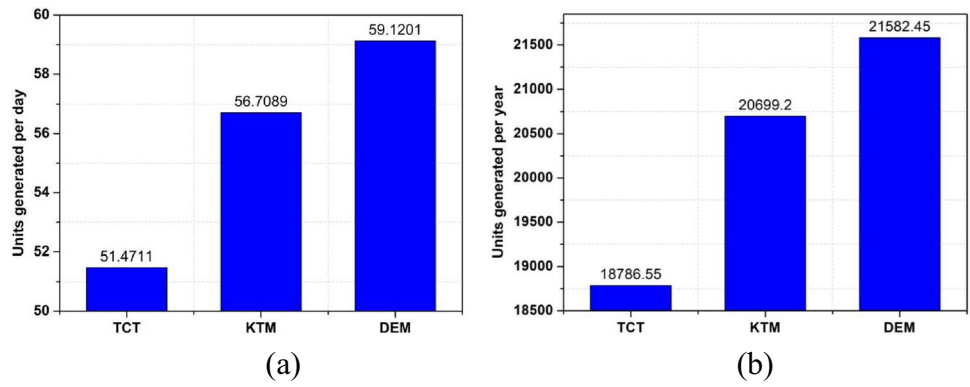


Table 7 A comparative economic analysis of TCT, KTM and DEM configurations

Array Config	hour	Pattern	GMP (W)	Hourly		Daily		Yearly	
				Units/hr (kWh)	Revenue /hr (Rs)	Units/day (kWh)	Revenue/day (Rs)	Units/year (kWh)	Revenue/year (Rs)
TCT	10–11	SB	7611	7.611	22.833	51.4711	154.413	18,786.55	56,360.74
	11–12	SN	8578.5	8.5785	25.7355				
	12–1	LB	6770.4	6.7704	20.3112				
	1–2	L	9200	9.2	27.6				
	2–3	Triangle	9943.2	9.9432	29.8296				
KTM	3–4	Rhombus	9368	9.368	28.104	56.7089	170.126	20,699.20	62,095.99
	10–11	SB	9521	9.521	28.563				
	11–12	SN	8871.8	8.8718	26.6154				
	12–1	LB	7851.1	7.8511	23.5533				
	1–2	L	9808	9.808	29.424				
DEM	2–3	Triangle	10,343	10.343	31.029	59.1201	177.361	21,582.45	64,740.05
	3–4	Rhombus	10,314	10.314	30.942				
	10–11	SB	9542	9.542	28.626				
	11–12	SN	9878.5	9.8785	29.6355				
	12–1	LB	8559.6	8.5596	25.6788				
	1–2	L	10,175	10.175	30.525				
	2–3	Triangle	10,659	10.659	31.977				
	3–4	Rhombus	10,306	10.306	30.918				

Fig. 27 (a) Revenue generated per day and (b) per year

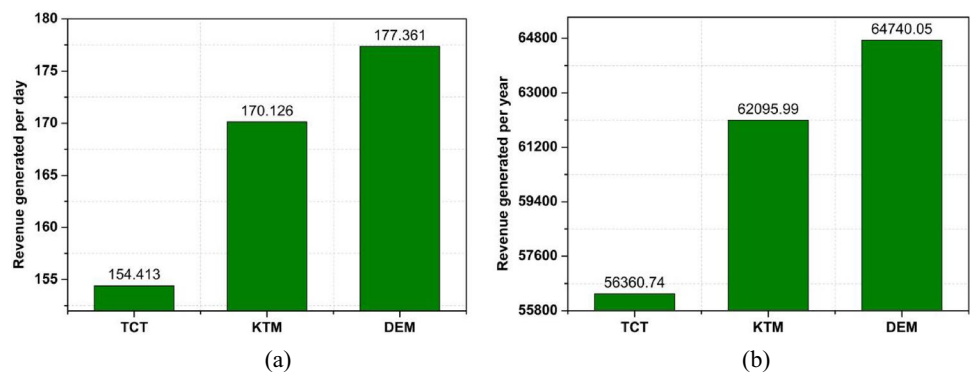
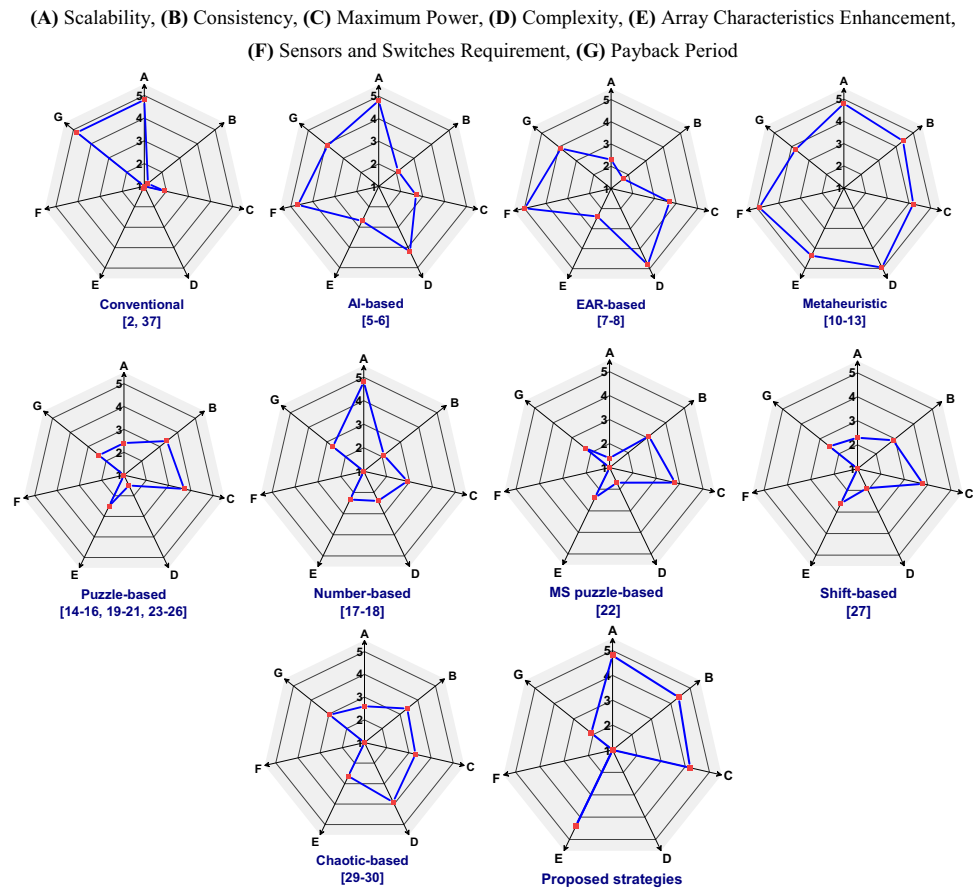


Fig. 28 Performance comparison of various strategies using different indices **(A)** Scalability, **(B)** Consistency, **(C)** Maximum Power, **(D)** Complexity, **(E)** Array Characteristics Enhancement, **(F)** Sensors and Switches Requirement, **(G)** Payback Period



- The proposed methods circumvent the shortcomings of population-based meta-heuristic optimization algorithms [10–13] such as high dimension search space, convergence & parameter selection issues, methodology challenges, being stuck at local optimum, weighting factor shortlisting difficulties, gigantic computations, heavy computational time, etc.
- The proposed approaches, in contrast with the current logic- and puzzle-based methodologies [14–16, 19–21, 23–26], are fully scalable and adaptable with all array sizes. Additionally, the proposed configurations evenly and effectively spread the shade over the array.
- The proposed reconfiguration strategies effectively address a number of shortcomings of the current magic square-based [22], shift-based [27], and index-based [28] methods, including inadequate scalability, a high association between the diagonal arrangement of panels, inconsistency, etc.
- The recent OE [17] and OEP [18] approaches, while adaptable to any array sizing, produce performance that is extremely inconsistent since the panels' poor placement after reconfiguration has a strong correlation between the next shaded panels row-wise. The proposed ones, in contrast, are consistently more efficient in shaded environments and are also generally compatible.

The overall comparison of the proposed techniques with the state of art techniques are shown in Fig. 28.

Conclusions

The GMP obtained by the PV array is mainly restrained due to PS. The proposed KTM and DEM reconfiguration techniques effectively disperses the shade thereby enhancing the GMP and lessening the mismatch losses. For the various shading conditions considered for symmetrical 8×8 array such as SB, SN, LB, L-shaped, triangle-shaped, rhombus-shaped, and square-shaped, the enhancement in GMP from TCT to DEM configuration is 25.38%, 15.16%, 26.43%, 10.59%, 7.19%, 10.02%, and 4.03% respectively, and the enhancement in GMP from TCT to KTM configuration is 25.09%, 3.42%, 15.97%, 6.61%, 4.03%, 10.09%, 4.03% respectively. Moreover, there is a significant improvement in the PV and IV characteristics as the number of bypasses are significantly reduced by the proposed techniques. By employing the proposed DEM and KTM techniques, the respective annual generated revenue is increased by 14.9% and 10.18% compared to benchmark TCT. Further, for the unsymmetrical 4×3 array, the enhancement in GMP of the

KTM configuration wrt TCT is 25.52%, 10.64%, 13.85%, 5.55%, 3.92% and the enhancement in GMP of the DEM configuration wrt TCT is 26.06%, 25.11%, 16.82%, 10.80%, 10.46%, 7.57%, 4.24% respectively. The existing OE and OEP configurations offer inconsistent and inferior performance compared to the proposed ones.

Hence, from the technical and economic analysis, it is exemplary to accept that both proposed techniques efficiently distribute the shadow over the entire array and are quite fitting to be exercised for both symmetrical and unsymmetrical PV arrays under PS. By increasing the ratings of PV panels, the output power is maximized thereby maximizing the revenue generated. Both the proposed DEM and KTM techniques outperformed the conventional TCT for all performance indices. Further, when compared to KTM, the DEM technique renders superior performance under most shading conditions and proves to be an effective solution for PS issues.

Data Availability Data sharing not applicable to this article as no datasets were generated or analysed during the current study.

Declaration

Competing Interest No potential competing interest was reported by the authors.

References

- Naik KA et al (2022) Generalized cryptographic image processing approaches using integer-series transformation for solar power optimization under partial shading. *Energy Convers Manag* 272:116376. <https://doi.org/10.1016/j.enconman.2022.116376>
- Raj RDA, Naik KA (2022) A novel scan pattern for reconfiguration of partially shaded photovoltaic arrays for maximum power extraction. *Int. J. Circuit Theory Appl.* <https://doi.org/10.1002/cta.3452>
- Yatimi H, Aroudam E (2018) MPPT algorithms based modeling and control for photovoltaic system under variable climatic conditions. *Procedia Manuf* 22:757–764. <https://doi.org/10.1016/j.promfg.2018.03.108>
- Raj RDA, Naik KA (2022) Optimal reconfiguration of PV array based on digital image encryption algorithm: a comprehensive simulation and experimental investigation. *Energy Convers Manag* 261:115666. <https://doi.org/10.1016/j.enconman.2022.115666>
- Solis-Cisneros HI, Sevilla-Camacho PY, Robles-Ocampo JB, Zuñiga-Reyes MA, Rodríguez-Resendiz J, Muñoz-Soria J, Hernández-Gutiérrez CA (2022) A dynamic reconfiguration method based on neuro-fuzzy control algorithm for partially shaded PV arrays. *Sustain. Energy Technol. Assess* 52:102147. <https://doi.org/10.1016/j.seta.2022.102147>
- Nguyen-Duc T, Le-Viet T, Nguyen-Dang D, Dao-Quang T, Bui-Quang M (2022) Photovoltaic Array reconfiguration under partial shading conditions based on short-circuit current estimated by convolutional neural network. *Energies* 15:6341
- Storey JP, Wilson PR, Bagnall D (2013) Improved optimization strategy for irradiance equalization in dynamic photovoltaic arrays. *IEEE trans. On power. Electronics* 28:2946–2956. <https://doi.org/10.1109/TPEL.2012.2221481>
- Zhu Z, Hou M, Ding L, Zhu G, Jin Z (2020) Optimal photovoltaic Array dynamic reconfiguration strategy based on direct power evaluation. *IEEE Access* 8:210267–210276. <https://doi.org/10.1109/ACCESS.2020.3036124>
- Karakose M, Baygin M, Murat K, Baygin N, Akin E (2016) Fuzzy based reconfiguration method using intelligent partial shadow detection in PV arrays. *Int. J. Comput. Intell.* 9(2):202–212. <https://doi.org/10.1080/18756891.2016.1150004>
- Kumar A, Rizwan M, Nangia U, Alaraj M (2021) Grey wolf optimizer-based Array reconfiguration to enhance power production from solar photovoltaic plants under different scenarios. *Sustainability* 13:13627
- Yang B, Zeng C, Li D, Guo Z, Chen Y, Shu H, Cao P, Li Z (2022) Improved immune genetic algorithm based TEG system reconfiguration under non-uniform temperature distribution. *Appl Energy* 325:11s9691. <https://doi.org/10.1016/j.apenergy.2022.119691>
- Yousri D, El-Saadany EF, Shaker Y, Babu TS, Zobaa AF, Allam D (2022) Mitigating mismatch power loss of series-parallel and total-cross-tied array configurations using novel enhanced heterogeneous hunger games search optimizer. *Energy Rep* 8:9805–9827. <https://doi.org/10.1016/j.egy.2022.07.153>
- Ajmal AM, Ramachandaramurthy VK, Naderipour A, Ekanayake JB (2021) Comparative analysis of two-step GA-based PV array reconfiguration technique and other reconfiguration techniques. *Energy Convers Manag* 230:113806. <https://doi.org/10.1016/j.enconman.2020.113806>
- Rani BI, Ilango GS, Nagamani C (2013) Enhanced power generation from PV array under partial shading conditions by shade dispersion using Su do Ku configuration. *IEEE Trans Sustain Energy* 4(3):594–601
- Krishna SG, Moger T (2019) Optimal SuDoKu reconfiguration technique for Total-cross-tied PV Array to increase power output under non-uniform irradiance. *IEEE Trans on Energy Conv* 34(4):1973–1984. <https://doi.org/10.1109/TEC.2019.2921625>
- Yadav AS, Mukherjee V (2018) Line losses reduction techniques in puzzled PV array configuration under different shading conditions. *Sol Energy* 171:774–783. <https://doi.org/10.1016/j.solener.2018.07.007>
- Yadav K, Kumar B, Swaroop D (2020) Mitigation of mismatch power losses of PV Array under partial shading condition using novel odd even configuration. *Energy Rep* 6:427–437. <https://doi.org/10.1016/j.egy.2020.01.012>
- Reddy SS, Yammani C (2020) Odd-even-prime pattern for PV array to increase power output under partial shading conditions. *Energy* 213:15. <https://doi.org/10.1016/j.energy.2020.118780>
- Vijayalekshmy S, Bindu GR, Iyer SR (2016) A novel zig-Zag scheme for power enhancement of partially shaded solar arrays. *Sol Energy* 135:92–102. <https://doi.org/10.1016/j.solener.2016.05.045>
- Nihanth MSS, Ram JP, Pillai DS, Ghias AMYM, Garg A, Rajasekar N (2019) Enhanced power production in PV arrays using a new skyscraper puzzle based one-time reconfiguration procedure under partial shade conditions (PSCs). *Sol Energy* 194:209–224. <https://doi.org/10.1016/j.solener.2019.10.020>
- Sagar G, Pathak D, Gaur P, Jain V (2020) A Su do Ku puzzle based shade dispersion for maximum power enhancement of partially shaded hybrid bridge-link-total-cross-tied PV array. *Sol Energy* 204:161–180. <https://doi.org/10.1016/j.solener.2020.04.054>
- Reddy SS, Yammani C (2020) A novel Magic-Square puzzle based one-time PV reconfiguration technique to mitigate

- mismatch power loss under various partial shading conditions. *Optik* 222:165289. <https://doi.org/10.1016/j.ijleo.2020.165289>
23. Venkateswari R, Rajasekar N (2020) Power enhancement of PV system via physical array reconfiguration based Lo Shu technique. *Energy Convers Manag* 215:112885. <https://doi.org/10.1016/j.enconman.2020.112885>
 24. Horoufiyany M, Ghandehari R (2018) Optimization of the Sudoku based reconfiguration technique for PV arrays power enhancement under mutual shading conditions. *Sol Energy* 159:1037–1104. <https://doi.org/10.1016/j.solener.2017.05.059>
 25. Tatabhatla VMR, Agarwal A, Kanumuri T (2019) Performance enhancement by shade dispersion of solar photo-voltaic array under continuous dynamic partial shading conditions. *J of Cleaner Production* 213:462–479. <https://doi.org/10.1016/j.jclepro.2018.11.015>
 26. Tatabhatla VMR, Agarwal A, Kanumuri T (2021) Performance improvement by mitigating the effects of moving cloud conditions. *IEEE Trans Power Electron* 36:4214–4223. <https://doi.org/10.1109/TPEL.2020.3020807>
 27. Madhanmohan VP, Nandakumar M, Saleem A (2020) Enhanced performance of partially shaded photovoltaic arrays using diagonally dispersed total cross tied configuration. *Recovery, Utilization, and Environmental Effects, Energy Sources A*. <https://doi.org/10.1080/15567036.2020.1826008>
 28. Pillai DS, Ram JP, Nihanth MSS, Rajasekar N (2018) A simple, sensorless and fixed reconfiguration scheme for maximum power enhancement in PV systems. *Energy Convers Manag* 172:402–417. <https://doi.org/10.1016/j.enconman.2018.07.016>
 29. Tatabhatla VMR, Agarwal A, Kanumuri T (2022) A Chaos map based reconfiguration of solar Array to mitigate the effects of partial shading. *IEEE Trans. Energy Convers.* 37:811–823. <https://doi.org/10.1109/TEC.2021.3122470>
 30. Raj RDA, Naik KA (2022) A generalized Henon map-based solar PV Array reconfiguration technique for power augmentation and mismatch mitigation. *IETE J Res.* <https://doi.org/10.1080/03772063.2022.2055660>
 31. Pendem SR, Mikkili S (2018) Modelling and performance assessment of PV array topologies under partial shading conditions to mitigate the mismatching power losses. *Sol Energy* 160:303–321. <https://doi.org/10.1016/j.solener.2017.12.010>
 32. Vinod KR, Singh SK (2018) Solar photovoltaic modeling and simulation: as a renewable energy solution. *Energy Rep* 4:701–712. <https://doi.org/10.1016/j.egy.2018.09.008>
 33. Raj RDA, Naik KA (2022) An image encryption concept based solar photovoltaic array reconfiguration techniques for mismatch mitigation. *Energy Sources* 44(1):951–972. <https://doi.org/10.1080/15567036.2022.2052383>
 34. Chia GL, Ong SH (2005) Generalized knight's tours on rectangular chessboards. *Discret Appl Math* 150:80–98. <https://doi.org/10.1016/j.dam.2004.11.008>
 35. Lin SS, Wei CL (2005) Optimal algorithms for constructing knight's tours on arbitrary $n \times m$ chessboards. *Discret Appl Math* 146:219–232. <https://doi.org/10.1016/j.dam.2004.11.002>
 36. Nordgren RP (2012) On properties of special magic square matrices. *Linear Algebra Appl* 437:2009–2025. <https://doi.org/10.1016/j.laa.2012.05.031>
 37. Chia GL (2018) Self-complementary magic squares of doubly even orders. *Discret Math* 341:1359–1362. <https://doi.org/10.1016/j.disc.2018.02.010>
 38. Raj RDA, Naik KA (2022) A novel solar photovoltaic Array reconfiguration technique using two-dimensional generalized Arnold's cat map. *ASME J Sol Energy Eng* 144(6):061001. <https://doi.org/10.1115/1.4054506>
 39. Amar Raj RD, Bhattacharjee S, Biswas M (2020) Electrical reconfiguration technique for partially shaded PV arrays with minimal interconnections. *2020 International Conference on Power Electronics & IoT Applications in Renewable Energy and its Control (PARC), Mathura, India* pp. 90–95. <https://doi.org/10.1109/PARC49193.2020.236564>
 40. Anang N, Azman SN, Muda WMW, Dagang AN, Daud MZ (2021) Performance analysis of a grid-connected rooftop solar PV system in Kuala Terengganu. *Malaysia, Energy and Buildings* 248:111182. <https://doi.org/10.1016/j.enbuild.2021.111182>

Publisher's Note Springer Nature remains neutral with regard to jurisdictional claims in published maps and institutional affiliations.

Springer Nature or its licensor (e.g. a society or other partner) holds exclusive rights to this article under a publishing agreement with the author(s) or other rightsholder(s); author self-archiving of the accepted manuscript version of this article is solely governed by the terms of such publishing agreement and applicable law.